



**HAL**  
open science

## $\pi$ -Conjugated Phospholes and their Incorporation into Devices; A Component with a Great Deal of Potential

Matthew P. Duffy, Wylliam Delaunay, Pierre-Antoine Bouit, Muriel Hissler

► **To cite this version:**

Matthew P. Duffy, Wylliam Delaunay, Pierre-Antoine Bouit, Muriel Hissler.  $\pi$ -Conjugated Phospholes and their Incorporation into Devices; A Component with a Great Deal of Potential. *Chemical Society Reviews*, 2016, 45 (19), pp.5296-5310. 10.1039/C6CS00257A . hal-01321238

**HAL Id: hal-01321238**

**<https://univ-rennes.hal.science/hal-01321238>**

Submitted on 25 May 2016

**HAL** is a multi-disciplinary open access archive for the deposit and dissemination of scientific research documents, whether they are published or not. The documents may come from teaching and research institutions in France or abroad, or from public or private research centers.

L'archive ouverte pluridisciplinaire **HAL**, est destinée au dépôt et à la diffusion de documents scientifiques de niveau recherche, publiés ou non, émanant des établissements d'enseignement et de recherche français ou étrangers, des laboratoires publics ou privés.

# $\pi$ -Conjugated Phospholes and their Incorporation into Devices; A Component with a Great Deal of Potential

M.P. Duffy,<sup>a</sup> W. Delaunay,<sup>a</sup> P-A. Bouit,<sup>a</sup> and M. Hissler<sup>a\*</sup>

This review serves as a brief introduction to phospholes and discusses their unique favorable properties for applications in organic electronic materials. Over the past several years,  $\pi$ -conjugated phospholes have been slowly making their way into devices. We report here the mode of synthesis for these  $\pi$ -conjugated phospholes as well as discuss the performances of the devices.

## Introduction

The field of organic electronics has been growing extremely fast due to its wide applicability in photovoltaics, photonics, and consumer electronics. These organic semiconductors (i.e. small molecules, oligomers, and polymers) are considered to be the future building blocks of lightweight, flexible, large-area, as well as low-cost electronic devices. The starting point for this growth began in the 1970's with the discovery of conductivity within organic crystals<sup>1</sup> as well as in doped polyacetylene polymers.<sup>2</sup> Over the years, many research teams started to develop new  $\pi$ -conjugated systems incorporating different aromatic rings, such as benzene<sup>3</sup> or heterocyclopentadienes (pyrrole<sup>4</sup>, furan<sup>5</sup>, thiophene<sup>6</sup>, silole<sup>7</sup>) into the oligomeric and polymeric backbone. These  $\pi$ -conjugated polymers and oligomers have emerged as promising materials to build electronic flexible devices like organic light emitting diodes (OLED), organic field effect transistors (OFET) or organic photovoltaic cells (OPV).<sup>8</sup>

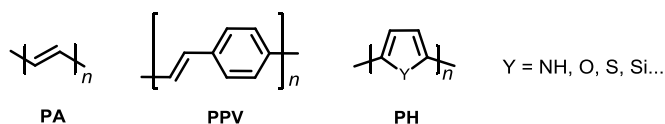


**Figure 1:** Examples of conjugated polymers. PA= polyacetylene, PPV = poly(phenylenevinylene), PH= polyheteroles.

In fact, the insertion of heteroatoms increases the stability of the  $\pi$ -conjugated systems. The poly(pyrrole) obtained by electropolymerization is one of the first examples of making conjugated systems from heteroles.<sup>4a</sup> Then, for several reasons (i.e. chemical stability, thermal stability, conductivity...), the polythiophenes have slowly become more studied over the years compared to the other systems, with the synthesis of many structures such as poly-3-hexylthiophene (P3HT) or poly(3,4-ethylenedioxythiophene) (PEDOT), which are very famous as active materials in OPVs,<sup>9</sup> OFETs,<sup>10</sup> and OLEDs.<sup>11</sup>

While organic electronics has extensively developed over

the years, it remains limited by the number of materials that are available. In order to further expand the field, new types of  $\pi$ -conjugated moieties or components need to be incorporated into the  $\pi$ -conjugated backbone of oligomers and polymers to find new classes of conjugated materials. Unlike the five-membered heterocyclic systems based on nitrogen, sulfur, or oxygen, which have been known for over 130 years and have been studied for decades, the system based on one phosphorus were discovered<sup>12</sup> 55 years ago and have been incorporated into  $\pi$ -conjugated systems only since the 90s.<sup>13</sup> The phosphole exhibits unique properties different from the other five-membered heterocyclic members making him it an interesting building block for the construction of  $\pi$ -systems having specific properties.<sup>14</sup> In this review, we will discuss phospholes, their synthesis, their unique properties useful for organic electronic materials, and the devices that they have been incorporated in so far.

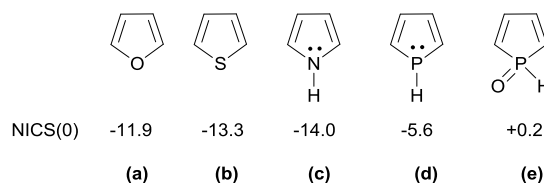


**Figure 2:** (a) Furan. (b) Thiophene. (c) Pyrrole. (d) 1H-Phosphole. (e) Phosphole oxide. Nucleus-Independent Chemical Shift (NICS)(0) values calculated at the B3LYP/cc-pVTZ level.<sup>15</sup>

The phosphole (a.k.a 1H-phosphole) is a five membered ring, consisting of a dienic system bridged with a phosphorus atom. It was first discovered in 1959, by two independent groups, as the 1,2,3,4,5-pentaphenylphosphole.<sup>12</sup> The parent 1H-phosphole (Figure 2, (d)) was characterized for the first time at low-temperature in 1983.<sup>16</sup> Therefore the late blooming of phosphole chemistry and their incorporation into  $\pi$ -conjugated systems is not surprising.<sup>17</sup>

The degree of aromaticity of the phosphole ring has been the subject of several experimental and theoretical studies.<sup>13a, 14, 18, 19</sup> The conclusion, based on energetic, structural, and magnetic criteria are that 1-H phospholes are very weakly aromatic. Using nucleus-independent chemical shift (NICS) calculations (B3LYP/cc-pVTZ) to measure the degree of aromaticity, where negative chemical shifts denote aromaticity and positive NICS antiaromaticity, phosphole has a NICS(0) = -

<sup>a</sup>Institut des Sciences Chimiques de Rennes, UMR 6226 CNRS-Université de Rennes1, Campus de Beaulieu, 35042 Rennes Cedex, France.

† Footnotes relating to the title and/or authors should appear here.

Electronic Supplementary Information (ESI) available: [details of any supplementary information available should be included here].

5.6, compared to thiophene (NICS(0) = -13.3) and pyrrole (NICS(0) = -14.0) which exhibit higher degrees of aromaticity.<sup>15</sup> Phospholes are only slightly more aromatic than cyclopentadiene (NICS(0) = -3.0).<sup>15</sup> The trigonal pyramidal shape of the tri-coordinate phosphorus atom, causes a non-planar conformation of the phosphole, where the phosphorus lone pair has inefficient interaction with the endocyclic dienic system (see Figure 3) thus the very large decrease in aromaticity. Theoretical calculations have shown that a planar phosphole would have a higher aromaticity than thiophene or pyrrole; however, the aromatic delocalization stabilization energy is insufficient to overcome the high energy barrier required to force the phosphorus atom to become planar.<sup>17e</sup>



**Figure 3:** (Left) pyrrole. (Right) phosphole.

The aromaticity of the phosphole is highly influenced by the nature of the substituents attached to the cycle, especially those directly linked to the phosphorus atom.<sup>13a, 18b, 18d, 18f, 20</sup> Phospholes bearing very bulky substituents (e.g. 2,4,6-tri-*tert*-butylphenyl) on the phosphorus are more planar and show a higher aromaticity as well as some electrophilic substitution reactivity.<sup>21</sup> If the P-substituent is an alkoxy or halogen, the phosphole loses most of the cyclic delocalization and readily undergoes [4+2] cycloadditions.<sup>18f, 20b</sup> These last observations can be explained by the presence of a hyperconjugation between the exocyclic P-R bond and the  $\pi$ -system of the dienic moiety.<sup>14,18f</sup> Thus, changing the substituent directly attached to the phosphorus could offer a modification in the way that the endocyclic diene (of the phosphole) participates within the  $\pi$ -conjugated backbone. The efficient  $\sigma$ - $\pi$  interaction offers an original mode of conjugation that can be further investigated for the synthesis of new  $\pi$ -conjugated materials.

Since most phospholes are only very weakly aromatic, they do not undergo facile electrophilic aromatic substitution reactions as other “aromatic” five-membered heterocycles do. This leads phospholes to have their own unique chemistry, and can make functionalization about the phosphole more challenging.<sup>13a, 22</sup> An easier approach for functionalization of the phosphole is to design the desired functional groups first by classical organic synthesis reactions and to generate the phosphole in the final step(s).<sup>20c,23</sup>

Further functionalization of the phosphole ring can be achieved via the phosphorus lone pair. Since the phosphorus lone pair has inefficient interaction with the endocyclic dienic system of the phosphole ring, the lone pair stays reactive to realize modifications such as oxidation (O, S, Se), alkylation (-CH<sub>3</sub>) or coordination toward a wide range of transition metals (W, Fe, Pd, Pt...). The chemical modifications of this lone pair widely influences the physicochemical properties of the compounds. For example, the oxidation of the lone pair of the phosphorus atom induces a positive shift by a several ppm of the NICS(0) value thus the phosphole’s weak aromaticity is

shifted towards a small antiaromaticity in the case of the phosphole oxide (Figure 2 (e)).<sup>18</sup> This behavior has been intensively studied by Réau/Hissler since 2000.<sup>24</sup> Thus by merely playing with coordination of the phosphorus lone pair one is able to tune optical and redox properties of the phosphole  $\pi$ -conjugated material without the need of several additional synthetic steps. A recent publication by Hissler/Réau/Bouit *et al.* demonstrates this tunability extremely visually (see Figure 4).<sup>25</sup>

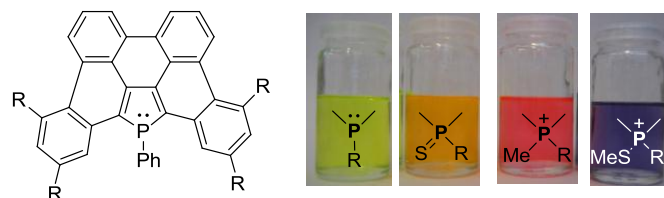


**Figure 4:** Coordination of the lone pair on a phosphole in a  $\pi$ -conjugated system allows the tunability of optical and redox properties.<sup>25</sup> Adapted with permission from ref. 25. Copyright 2012 American Chemical Society

Thus, phospholes contain unique favorable properties that have several applications in organic electronic materials; (i) phospholes are weakly aromatic, which favors the electronic delocalization in extended  $\pi$ -conjugated systems, (ii) substituents about the phosphole, especially those directly linked to the phosphorus atom can influence the aromaticity of the phosphole and have an effect on the properties of the  $\pi$ -system. Effectively, an efficient overlap between the  $\sigma$  orbitals of the exocyclic P-R bond and the  $\pi$ -orbitals from the endocyclic dienic system, offers an original mode of conjugation for phosphole  $\pi$ -conjugated systems, (iii) phospholes contain a reactive phosphorus atom, which offers the possibility to tune the physicochemical properties (wavelength of absorption/emission, electrochemical properties, thermal/chemical stability...) by using easy chemical modifications (oxidation, alkylation, coordination...), (iv) the pyramidal shape of the P-atom affords steric hindrance that prevents  $\pi$ -stacking in the solid state and thus promotes solid-state emission.

The last two properties mentioned are general for phosphanes,<sup>26</sup> but the others are typical of the phosphole ring, which makes them unique building blocks for the preparation of  $\pi$ -conjugated systems. The following section will describe the state of the art work that has been realized with phosphole derivatives, focusing on  $\pi$ -conjugated systems that have been inserted into devices.

### Organic light emitting diodes (OLED)

OLEDs based on organic polymers or small molecules have attracted much attention due to their potential use in a variety of applications such as flat-panel displays and solid-state lighting.<sup>27</sup> The basic multilayer structure of an OLED, shown in Figure 5, includes several layers (a transparent conducting oxide anode, a hole-transport layer (HTL), an emissive layer (EML), an electron transport layer (ETL), and a metallic low work function cathode), all playing a specific role in the production of light *via* electroluminescence (EL).<sup>27,28</sup>

Under forward bias, the HTL is *oxidized* as holes are injected from the anode into the highest occupied molecular orbital (HOMO) of the HTL, and the ETL is *reduced* as electrons are injected from the cathode into the lowest unoccupied molecular orbital (LUMO) of the ETL. Then, these charge carriers migrate under the applied electric field and recombine to form singlet and triplet excitons (bound excited-state electron-hole pairs) within the EML, which can return to the ground state *via* a radiative decay pathway.

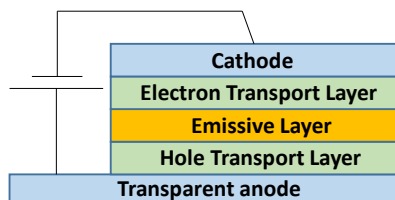


Figure 5 : OLED structure

For an organic material to be suited for OLED applications, the material must fulfill certain requirements: (i) the material should (i) be highly emissive (fluorescent or phosphorescent) in the solid state, (ii) be thermally stable, (iii) have suitable redox potentials for charges to be injected, (iv) be stable under electric fields, (v) exhibit both electron and hole transporting properties in order to favor exciton formation, and (vi) be able to give homogeneous layers (e.g. by either spin coating or via vacuum deposition). Since the scientists have been able to exploit the flexibility available for fine-tuning of the chemical, optical and electrochemical properties of phosphole-based conjugated systems through manipulation of their chemical structure, the phosphole-based oligomers and polymers have been successfully incorporated in OLED structure

### Phosphole based OLEDs

In 2003, in a short communication, Réau/Hissler *et al.* realized the first insertion of a  $\pi$ -conjugated phosphole derivative into an OLED device.<sup>29</sup> They described three different fluorophores based on a thiophene-phosphole-thiophene structure: **1a** with the free lone pair on the phosphorus, **2a** an oxidized version with sulfur, and **3a** a gold (I) complex (Figure 6). The mode of synthesis for these symmetrical  $\pi$ -conjugated phospholes starts with a Sonogashira<sup>30</sup> reaction of a haloarene with 1,7-octadiyne, followed by the Fagan-Nugent<sup>31</sup> method for generation of the phosphole.

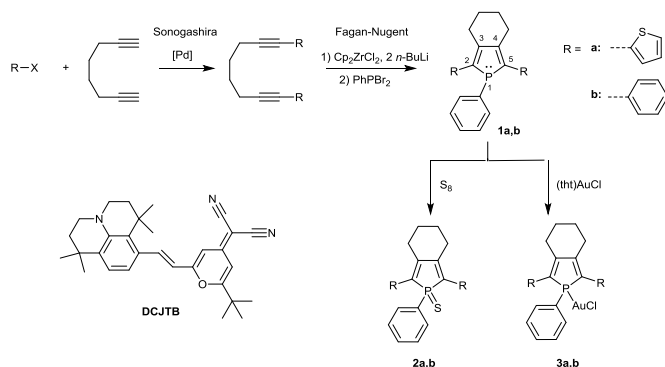
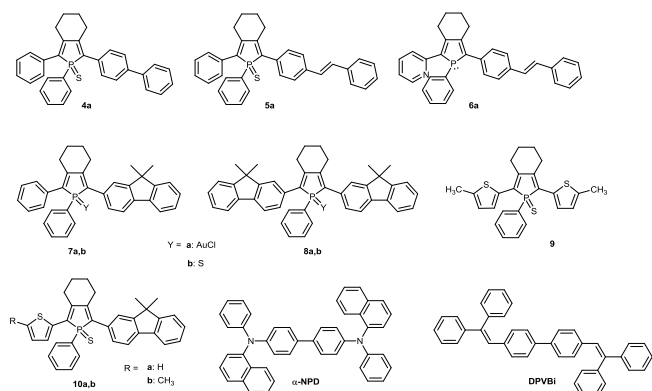


Figure 6: First phospholes inserted into an OLED device as well as guest used.

The first devices in the study had the following configuration: [ITO/PEDOT:PSS/organic layer/Mg:Ag/Ag]. The different organic layers were deposited by thermal evaporation under high vacuum. This procedure leads to the decomposition of  $\lambda^3, \sigma^3$ -phosphole **1a** but the thermal stability of the thioxo derivative **2a** and the gold (I) complex **3a** (Figure 6) allowed the ability to get homogeneous thin films. The emission wavelength of the thin film of **2a** is centered at 542 nm and very close to what was obtained in a THF solution (548 nm). Furthermore, the EL of the device containing **2a** is approximately constant up to high current ( $600 \text{ mA cm}^{-2}$ ), indicating a good operating stability. However, the maximum brightness (MB) ( $3,600 \text{ cd m}^{-2}$ ) and the external quantum yield (EQE) ( $\eta_{\text{max}} = 0.16$ ) was low, most likely due to unbalanced carrier injection or transport. Because single-layer OLEDs usually give poor efficiency and brightness, due to the fact that electroluminescent organic materials tend to have either n-type (electron-transport) or p-type (hole-transport) charge-transport characteristics, they decided to build multi-layered OLEDs using (tris-(8-hydroxyquinoline) aluminium ( $\text{Alq}_3$ ) as an ETL and (N,N'-diphenyl-N,N'-bis(1-naphthyl)-(1,1'-biphenyl)-4,4'-diamine ( $\alpha$ -NPD) as a HTL. In this multi-layered device [device configuration: ITO/PEDOT:PSS/ $\alpha$ -NPD/organic layer/ $\text{Alq}_3$ /Mg:Ag/Ag], the performance of the devices were improved, with the device incorporating phosphole **2a** (Figure 6) having the best performance ( $\lambda_{\text{max}} = 550 \text{ nm}$ , MB =  $38,000 \text{ cd m}^{-2}$ ,  $\eta_{\text{max}} = 0.80$ ). To improve the OLED performance, and to modify the color emitted, an appealing method is to dope highly fluorescent dyes as guests into an emissive host matrix. They tried this approach with phosphole derivative **2a** as the host and the highly red fluorescent dye 4-(dicyanomethylene)-2-tert-butyl-6-(1,1,7,7-tetramethyl-julolidin-4-yl-vinyl)-4H-pyran (DCJTBA, Figure 6) as the emitting guest. Although the dopant concentration (1.4 % wt) was not optimized, there was an enhancement of the EQE ( $\eta_{\text{max}} = 1.83$ ) and a maximum brightness of  $37,000 \text{ cd/m}^2$  ( $\lambda_{\text{max}} = 617 \text{ nm}$ ) was reached.

Later in 2006, in a full article, Réau/Hissler *et al.* expanded their investigation with a range of phosphole derivatives with different substituents in the 2- and 5- positions of the phosphole as well as different chemical modifications on the phosphorus atom (**2a,b**; **3a,b**; **4-6a**, Figures 6 and 7).<sup>32</sup> The mode of synthesis for these symmetrical and unsymmetrical  $\pi$ -conjugated phospholes is the same as previously mentioned (Figure 6).



**Figure 7:** Phosphole derivatives used as emitter in OLEDs as well hosts used.

They described the photophysical, electrochemical, and optoelectronic properties of  $\pi$  conjugated systems incorporating phosphole moieties.<sup>32</sup> The variation of the substitution pattern of phospholes and chemical modification of their P atoms afford thermally stable derivatives **2a,b**, **3a,b**, **4a**, **5-6a** (Figure 6 and 7), which are photo- and electroluminescent. The comparison of the optical properties of a solution and a thin film of thioxophospholes **2a,b** and **4-5a** shows that these compounds do not form aggregates in the solid state. This property, which is also, supported by an x-ray diffraction study of these derivatives, results in an enhancement of the fluorescence quantum yields in the solid state. In contrast, (phosphole)gold(I) complexes **3a,b** exhibit a broad emission in thin film, which is due to the formation of aggregates. Single- and multilayer OLEDs using these P derivatives as the EML were fabricated. The emission color of these devices and their performances vary with the nature of the P material. These observations are also supported by another work published by Réau/Hissler *et al.* In 2010, they decided to change the substituents in the 2- and 5- positions of the phosphole. They incorporated moieties known for their fluorescent properties: fluorenes (Figure 7).<sup>33</sup> Once again they synthesized the derivatives from Sonogashira<sup>30</sup> reactions of haloarenes with 1,7-octadiyne, followed by the Fagan-Nugent method<sup>31</sup> (Figure 6) for generation of the phosphole. The devices had the following configuration [ITO/CuPc/ $\alpha$ -NPD]/organic layer/DPVBi/BCP/Alq<sub>3</sub>/LiF/Al] (BCP, bathocuproine, is used as a hole-blocking layer to avoid emission from Alq<sub>3</sub>). When the gold complexes, **7a** and **8a** (Figure 7) have been incorporated into the device structure, they did not perform too well and the devices had extremely short lifetimes. The reason for the poor performance was believed to be due to a fast decomposition of the phosphole gold complexes when an electric field was applied. On the other hand the phosphole sulfide derivatives, **7b** and **8b** (Figure 7), had low operating voltages (6.3 and 4.3 V, respectively) and much higher brightness than their gold complexed analogues. The device with **8b** as the active layer had the best performance with EQE of 1.8% and a power efficiency of 1.4 lm W<sup>-1</sup> (CIE coordinates (0.43, 0.53). This is the highest EQE reported for an OLED featuring phosphole as single component in the EML.

In 2009, Réau/Hissler *et al.* showed that the emitting  $\pi$ -conjugated phosphole derivatives can be used as dopants in a blue-light emitting host to construct efficient white organic light-emitting diodes (WOLEDs).<sup>34</sup> These mixed phosphole-thiophene oligomers (**1-2a**, Figure 6) generally emit light in the orange region of the electromagnetic spectrum and since white-light emission could potentially be obtained by combining orange and blue emissions, they chose a highly efficient blue emitter 4,4'-bis(2,2'-diphenylvinyl)biphenyl (DPVBi, Figure 7) as the host material. It is important to note that, the absorption spectra of phosphole-thiophene derivatives span the 320-524 nm range, and overlap with the emission spectrum of DPVBi to a large extent, potentially allowing energy transfer from the DPVBi host to the phosphole dopants. They constructed devices where DPVBi and phosphole-based dopants were coevaporated, in different ratios (doping rates < 1%), to generate the EML in the OLED device [device configuration: ITO/CuPc/ $\alpha$ -NPD/doped DPVBi/Alq<sub>3</sub>/LiF/Al] (CuPc: copper phthalocyanine). Construction of a device with a ratio of DPVBi: **2a** (0.2%), did in fact achieve a WOLED (CIE coordinates (0.305, 0.391) close to pure white light. The device had a turn on voltage of 5.2V, EQE of 2.7%, current efficiency of 7.0 cd A<sup>-1</sup>, and power efficiency of 2.3 lm W<sup>-1</sup>. Decreasing the ratio of DPVBi: **2a** (0.1%), achieved a whiter light from the WOLED, but having such a low doping rate (0.1%) is quite difficult to control and to reproduce in the coevaporation process. To circumvent this problem, they doped the  $\alpha$ -NPD layer (Figure 7) with **2a** (0.25%), and got a similar EL performance, with doping rates that could be more easily controlled and reproduced. However, **2a** was not sufficiently red-shifted enough to obtain an OLED that emitted pure white light. Thus phosphole **9** (Figure 7), which has a more red-shifted photoluminescence (PL) emission, was used as a dopant for the  $\alpha$ -NPD layer. A ratio of  $\alpha$ -NPD: **9** (0.2%), achieved an emission (CIE coordinates (0.282, 0.306)) closest to that of pure white light, the device had a turn on voltage of 5.2V, EQE of 3.6%, current efficiency of 7.8 cd A<sup>-1</sup>, and power efficiency of 2.0 lm W<sup>-1</sup>. The brightness of this optimized WOLED increased linearly with the current density. The brightness obtained with this device was 3,200 cd m<sup>-2</sup> for a current density of 50 mA cm<sup>-2</sup>.

Later, their structures were modified by replacing the phenyl group in the 2-position of the phosphole (**7b**) with a thiophene to give thermally stable and emissive phosphole derivatives **10a,b** (Figure 7), in an attempt to find new  $\pi$ -conjugated phospholes to be used for WOLEDs.<sup>35</sup> Although the structures **10a,b** appear very similar, they exhibited very different doping properties in a DPVBi host matrix. Using the device configuration [ITO/ CuPc/  $\alpha$ -NPD/ doped-DPVBi/ BCP/ Alq<sub>3</sub>/ LiF /Al], they doped DPVBi with different doping ratios of **10a**. They found that small variations of the doping ratio of **10a** had a large impact on both the CIE coordinates and on the external quantum yields of the devices, which is often classically observed. The best performing device, which displayed CIE coordinates (0.27, 0.33) close to pure-white emission, was with a doping ratio of 0.3% of **10a** in DPVBi. It had a turn-on voltage of 4.7V, brightness of 832 cd m<sup>-2</sup>, EQE of

2.1%, power efficiency of  $1.3 \text{ lm W}^{-1}$ , and a current efficiency of  $4.3 \text{ cd A}^{-1}$ . However, once again having such a low doping ratio value (0.3%) to reach white emission is difficult to control and reproduce in the coevaporation process. Using the same device configuration, but this time with **10b** (Figure 7) as the dopant, they found that when they increased the doping ratio of **10b** in DPVBi from 1% to 50%, although the CIE coordinates progressively changed, the EQE remained stable ( $2.4 \pm 0.1\%$ ). This unusual behaviour showed that **10b** was a quench-resistant dopant, unique for DPVBi. Although none of the devices exhibited pure-white emission, due to the fact that **10b** did not emit the exact complementary color of the DPVBi matrix, a doping rate for **10b** of 3.2% exhibited whitish emission (CIE coordinates, (0.32, 0.40)) had a turn on voltage of 5.6V, brightness of  $1,061 \text{ cd m}^{-2}$ , EQE of 2.3%, power efficiency of  $1.6 \text{ lm W}^{-1}$ , and a current efficiency of  $5.4 \text{ cd A}^{-1}$ .

Hissler *et al.*, recently showed that flexible OLEDs (or FOLEDs) could also be made with  $\pi$ -conjugated phospholes, by substituting the glass substrate for a poly(ethylene terephthalate) (PET) substrate.<sup>36</sup> Using phosphole **10b** (1.4%) in a DPVBi matrix, they constructed a device with the following configuration [PET/ ITO/ CuPc/  $\alpha$ -NPD/ doped-DPVBi/ Alq<sub>3</sub>/ LiF/ Al]. The flexible device with a bluish white emission (CIE coordinates, (0.18, 0.25)) had a small turn-on voltage 4.8V, brightness of  $2915 \text{ cd cm}^{-2}$ , power efficiency of  $1.9 \text{ lm W}^{-1}$ , a current efficiency of  $6.3 \text{ cd A}^{-1}$ , and an EQE of 2.3%. The device performance on the PET substrate was very similar to its glass counterpart.

In 2012, Hissler/Réau/Duan/Mathey *et al.* incorporated a  $\pi$ -conjugated 2,2'-biphosphole into a DPVBi matrix to generate a WOLED.<sup>37</sup> The 2,2'-biphosphole oligomers were synthesized using a method discovered by Mathey *et al.*<sup>38</sup> and then later developed by Gouyguo *et al.*<sup>39</sup> (Figure 8). When 1-aryl-3,4-dimethylphospholes are subjected to prolonged heating they undergo a tetramerization with migration of the aryl substituent. Next Na/naphthalene cleaves the P-P bonds to generate bisanionic species which is then alkylated with either MeI or Br(CH<sub>2</sub>)<sub>3</sub>Br. Subsequently the 2,2'-biphospholes are either oxidized or coordinated to give the desired products.

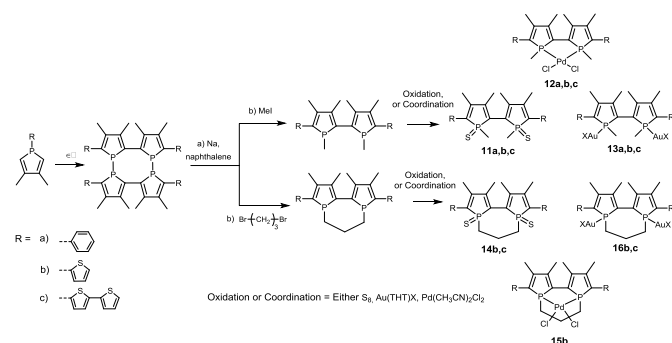


**Figure 8:** Generation of  $\pi$ -conjugated 2,2'-biphospholes.

The authors demonstrated that by changing the torsional angle between the biposphole, by the use of covalent bonding and/or metal coordination, they could tune the HOMO-LUMO gap of

the  $\pi$ -system. The 2,2'-biphosphole **14c** (Figure 8) was found to give an emission complementary to that of DPVBi, and have suitable HOMO and LUMO energies to be incorporated into an OLED device. It was thus used as a dopant for the development of a WOLED. The device [ITO/ CuPc/  $\alpha$ -NPB/ DPVBi:dopant 2.2%/ DPVBi/ Alq<sub>3</sub>/ LiF/ Al] exhibited satisfying performances (turn-on voltage 5.1V, brightness  $189 \text{ cd m}^{-2}$ , EQE of 0.5%, power efficiency  $0.31 \text{ lm W}^{-1}$ , current efficiency  $0.96 \text{ cd A}^{-1}$ ) and emitted white emission (CIE coordinates (0.34, 0.34)).

All the examples, shown so far, of emissive phospholes used for OLED applications have been with the phosphole ring in conjugation with other  $\pi$  systems. Another way of extending the delocalization of the  $\pi$  system is to fuse the phosphole directly into the  $\pi$ -conjugated system.

In 2012 Yasuda/Adachi *et al.* synthesized a series of heteroannulated (Si, P, S, and Ge)  $\pi$ -conjugated dithieno[3,2-*b*:2',3'-*d*]metallole derivatives, which included a dithieno[3,2-*b*:2',3'-*d*]phosphole (Figure 9), and examined their photophysical and electroluminescent properties, as well as incorporated the highly fluorescent compounds into OLEDs.<sup>40</sup> Using a previously reported procedure by Baumgartner *et al.*,<sup>41</sup> they synthesized the product by first performing a lithium-halogen exchange with 3,3'-dibromo-2,2'-dithiophene followed by addition of dichlorophenylphosphine (PhPCl<sub>2</sub>) to generate the dithieno[3,2-*b*:2',3'-*d*]phosphole. Next a bromination reaction is performed with *N*-bromosuccinimide (NBS) to give the dibrominated species, which in the presence of oxygen forms the phosphole oxide derivative. Finally, Suzuki coupling with phenylboronic acid afforded the  $\pi$ -conjugated phosphole **17** (Figure 9).

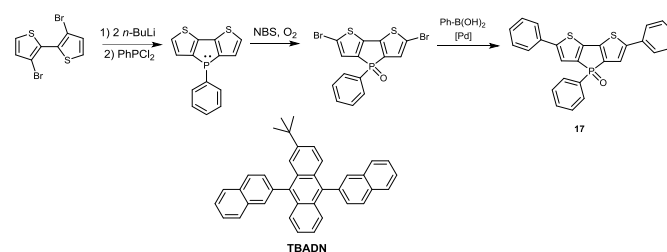


**Figure 9:** Synthesis of a dithieno[3,2-*b*:2',3'-*d*]phosphole **17**, and TBADN host used for the device.

The device constructed had the following configuration: [ITO/  $\alpha$ -NPD (HTL)/3 wt% emitter:TBADN/bathophenanthroline, (BPhen, ETL)/LiF/Al]. The device had a turn on voltage of 2.8V, maximum brightness of  $43,800 \text{ cd m}^{-2}$ , and EQE of 4.0%, with CIE coordinates (0.29,0.57). The only other device to have a slightly higher brightness ( $46,300 \text{ cd m}^{-2}$ ) was the device incorporating the sulfur derivative (dithienothiophene-*S*,*S*-dioxide).

In 2013, Réau/Hissler/Mathey *et al.* described the synthesis and the self-assembling properties in the solid state of benzofuran-fused phospholes **18** (Figure 10).<sup>42</sup>

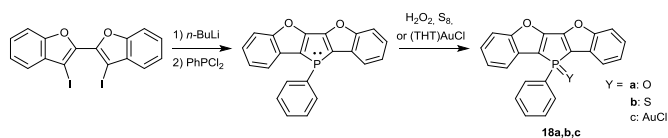


**Figure 10:** Benzofuran-fused phosphole derivatives for OLEDs.

They were synthesized by reacting the (bis)iodo-substituted benzofuran with 2 equivalents of *n*-BuLi and one equivalent of PhPCl<sub>2</sub> at -78°C to generate the phosphole, followed by oxidation or complexation to give **18a,b,c** (Figure 10). Taking into account thermal stabilities and physical properties of these derivatives, compound **18a** was used as an emitting material, either as the pure EML or doped in a DPVBi matrix, for OLED devices. Using the device configuration [ITO/CuPc/ $\alpha$ -NPD/EML/DPVBi/BCP/Alq<sub>3</sub>/LiF/Al], compound **18a** was first used as a pure emitter, but the brightness and EQE were moderate and due to aggregation of the molecules in solid state, the maximum emission wavelength was red-shifted compared to one measured in solution. However, when **18a** was used as a dopant (doping rate = 3.6%) in a DPVBi matrix, they obtained an OLED that emitted in the blue-green region (CIE coordinates, (0.22,0.43)), the characteristic emission properties of the molecule **18a**. The device had a turn on voltage of 5.70V, brightness of 1248 cd cm<sup>-2</sup>, EQE of 2.29%, and a power efficiency of 1.55 lm W<sup>-1</sup>.

In 2015 Ye/Lu *et al.* decided to enrich the family of fused phosphole systems and generate indole-fused phospholes and uncover their structure-property relationship.<sup>43</sup> Starting from 3,3'-dibromo-1,1'-dimethyl-1*H*,1'*H*-2,2'-biindole **19** (Figure 11), they performed the phosphole ring forming reaction with PhPCl<sub>2</sub>, catalyzed by *n*-BuLi, followed by oxidation with H<sub>2</sub>O<sub>2</sub>, to generate **20** (Figure 11). The bromination of **21** with NBS, yielded **22**, which could be transformed into **23** via a similar ring-forming reaction (Figure 11).

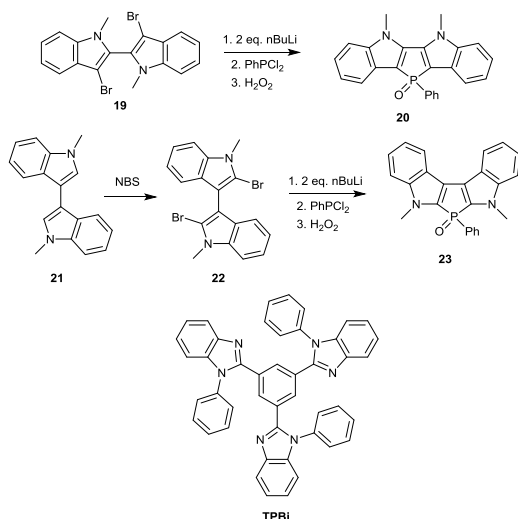


**Figure 11:** Synthesis of indole-fused phosphole systems **21** and **24**, and ETL used for OLED fabrication.

Since **20** and **23** (Figure 11) were emissive in the solid state, they have been used as emitters in OLEDs. They fabricated the

OLEDs with the following configuration [ITO/ $\alpha$ -NPD/emitter/TPBi/LiF/Al] where TPBi stands for 2,2',2''-(1,3,5-Benzinetriyl)-tris(1-phenyl-1*H*-benzimidazole) and is used as the electron-transporting layer. The device incorporating **20**, as an emitter, had the best performance, on account of its strong emission in the solid state compared to **23**. The device gave an emission centred at 540 nm, had a turn-on voltage of 1.5V, maximum brightness of 2636 cd m<sup>-2</sup>, maximum current efficiency 1.59 cd A<sup>-1</sup>, and a maximum power efficiency of 1.35 cd W<sup>-1</sup>. Although the OLED performance is moderate, this highlights another example of  $\pi$ -conjugated phosphole perspectives for OLEDs.

In 2012, Hissler/Réau/Bouit *et al.* synthesized the first fully planarized phosphorus containing polycyclic aromatic hydrocarbons (PAH), (e.g. **27** and **28**, Figure 12).<sup>25</sup> Recently they showed that these systems could be used to generate WOLEDs.<sup>44</sup> The phosphole were synthesized through the Fagan-Nugent method with dialkyne **24**, followed by thiooxydation/oxidation to give phospholes **25** and **26**, respectively (Figure 12). Next a photocyclization of **25** was performed to afford the PAH **27** (Figure 12). PAH **27** was further deprotected and oxidized to afford oxophosphole **27**, as direct photocyclization of **26** into **28** was inefficient (Figure 12). Contrary to the previous examples, the P atom is here introduced first and the planar backbone is then constructed around the P-heterocycle. Since these compounds are highly emissive in solution and possess suitable redox properties, they were used as orange dopant in a blue emitting matrix for the development of WOLEDs.

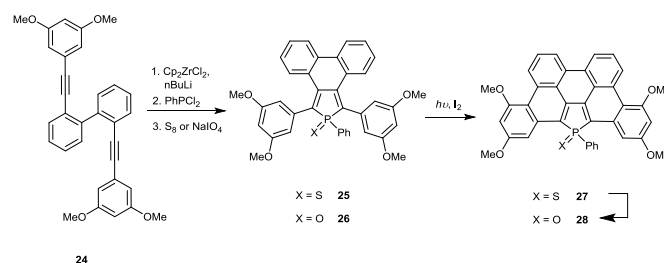


**Figure 12:** Synthesis of P-containing PAHs for use in WOLEDs.

The multilayered OLEDs had the following configuration [ITO/CuPc/ $\alpha$ -NPD/EML/DPVBi/BCP/Alq<sub>3</sub>/LiF/Al] and the EML was generated by co-subliming either **27** or **28** with the  $\alpha$ -NPD. The EL spectrum of the devices presents the dual emission of a blue-emitting matrix and the phosphorus-based dopant leading to a white emission as evidenced by the CIE coordinates. Effectively, the device utilizing emitter **28** in the emissive layer (EL =  $\alpha$ -NPD: **28** (0.8 wt%)) had a turn-on voltage of 6.06 V, brightness of 728 cd m<sup>-2</sup>, EQE of 1.19%, power efficiency of 0.61 lm W<sup>-1</sup>, current efficiency of 2.40 cd A<sup>-1</sup>, and with CIE coordinates (0.32, 0.35). The device utilizing emitter **27** in the emissive layer (EL =  $\alpha$ -NPD: **27** (1.1 wt%)) had a turn-on voltage of 5.55V, brightness of 1122 cd m<sup>-2</sup>, EQE of 1.67%, power efficiency of 0.96 lm W<sup>-1</sup>, current efficiency of 3.69 cd A<sup>-1</sup>, and with CIE coordinates (0.32, 0.37). The authors showed

that they could increase the performance of the device by changing the ETL ( $\text{Alq}_3$ ) and the hole-blocking layer (BCP) with TPBi. Under the new configuration [ITO/CuPc/ $\alpha$ -NPD/EML/DPVBi/TPBi/LiF/Al], the device incorporating **28** (EL =  $\alpha$ -NPD: **28** (1.2 wt%)) had a turn-on voltage of 5.19V, brightness of 1308  $\text{cd m}^{-2}$ , EQE of 2.10%, power efficiency of 1.40  $\text{lm W}^{-1}$ , current efficiency of 4.40  $\text{cd A}^{-1}$ , and with CIE coordinates (0.29, 0.34).

Huang *et al.* showed that  $\pi$ -conjugated phospholes incorporated into polymers, could be used to generate OLEDs. In 2006, Hissler/Réau *et al.* synthesized dibenzophosphole derivatives **29** (Figure 13) and described their photophysical, electrochemical, and optoelectronic properties.<sup>32</sup> They showed that dibenzophosphole derivatives **29** (Figure 13) are not suitable materials for OLEDs due to their weak PL in the solid state and the instability of the devices. In contrast, Huang *et al.* reported the synthesis of phosphafluorene (a.k.a. dibenzophosphole) copolymers (**30** and **31**, Figure 13) and then subsequently used the polymers as the EML in a polymeric light-emitting diode (PLED) device.<sup>45</sup> They formed the phosphole through low temperature Li/halogen exchange followed by a reaction with a dichlorophosphorus species. Subsequently, they used Suzuki coupling conditions to synthesize a copolymer where the phosphorus of the phosphole exists in the trivalent state with the free lone pair **30** and a copolymer where the phosphorus is pentavalent and protected by oxygen **31**.

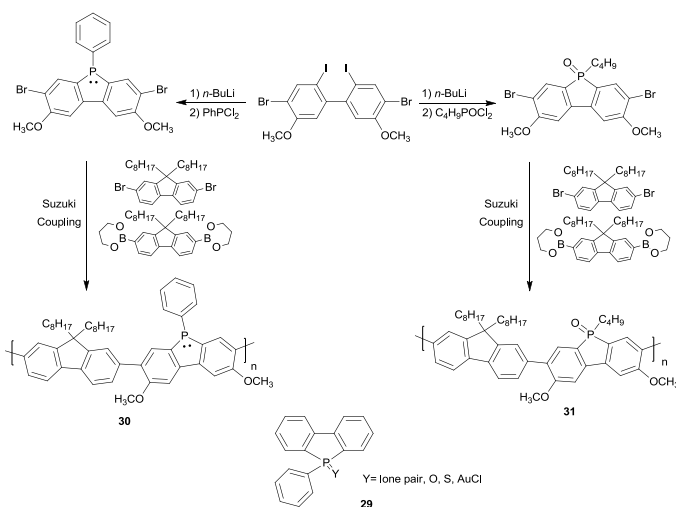


**Figure 13:** Phosphofluorene copolymers used for PLEDs and dibenzophospholes.

For copolymer **30**, the number-average molecular weight ( $M_n$ ) was 15,400, weight-average molecular weight ( $M_w$ ) was 35,800, the polydispersity index ( $M_w/M_n$ ) was 2.3, and the composition of the phosphole-fluorene derivative within the polymer was 7%. For copolymer **31**, the number-average molecular weight ( $M_n$ ) was 9,500, weight-average molecular weight ( $M_w$ ) was 10,200, the polydispersity index ( $M_w/M_n$ ) was 1.1, and the composition of the phosphole-fluorene derivative within the polymer was 11%. Both polymers were emissive and

had high decomposition temperatures (400°C). The copolymers were inserted into a device [configuration: ITO/ PEDOT:PSS/ polymer/ Ba/ Al]. The device with **30** as the EML, presented a blue EL (CIE coordinates: (0.21, 0.24)), and a brightness of 1423  $\text{cd m}^{-2}$ . When they incorporated **31** as the EML, the device showed white-light emission (CIE coordinates: (0.34, 0.36), although with much less brightness 142  $\text{cd m}^{-2}$ . The modification of the phosphole-fluorene derivative from the lone pair to the oxide significantly changed the properties of the polymer, changing the blue EL to a white one.

### Phosphole based electron-transporting layer for OLEDs

Tsuji/Sato/Nakamura *et al.* had a different take on the incorporation of a  $\pi$ -conjugated phosphole into an OLED.<sup>46</sup> Instead of using the phosphole derivative as the EML, they used their benzo[*b*]phosphole sulfides **32b** (Figure 14) as an ETL in an OLED.

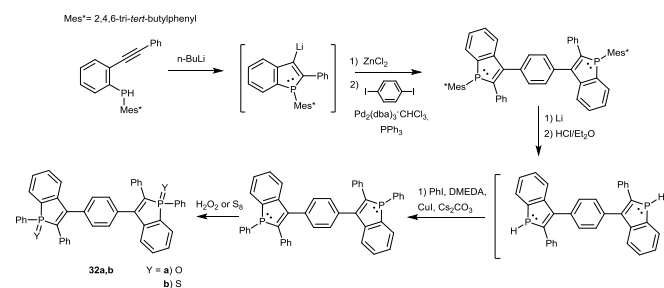


**Figure 14:** Synthesis of benzo[*b*]phospholes for use as electron-transporting layer in OLEDs.

The electron-transporting layer (ETL), as the name implies, helps to transport electrons from the cathode into the emitting layer. The requirements for an ETL include: (i) high electron transport mobility, (ii) reversible electrochemical reduction with a high reduction potential, (iii) appropriate energy levels with respect to the emitter to diminish the barrier for electron injection, (iv) thermally stability with high glass transition temperatures, and (v) the ability to form uniform, pinhole-free films (e.g. via vacuum deposition, spin casting, etc.).

Through a multi-step synthesis (Figure 14), Tsuji/Sato/Nakamura *et al.* were able to synthesize benzo[*b*]phosphole oxides<sup>43</sup> **32a** and sulfides<sup>42</sup> **32b**. When they first synthesized benzo[*b*]phosphole oxide **32a** and tested its electron mobility, they found it to be very low ( $5 \times 10^{-6} \text{ cm}^2 \text{ V}^{-1} \text{ s}^{-1}$ ).<sup>47</sup> They reasoned that the P=O sections of the molecule are so polarized that they could trap electrons, hindering the electron mobility. Their idea was to decrease the polarity (from P=O to P=S), and therefore possibly increase the electron mobility of the material. When they tested the electron mobility of the 1:1 diastereomeric mixture (due to the chirality of the 2 phosphorus atoms) of **32b**, they found it to be a good *n*-type material, with an electron mobility of  $2 \times 10^{-3} \text{ cm}^2 \text{ V}^{-1} \text{ s}^{-1}$ , which at the time was among the highest found for amorphous organic materials. They tested the devices using either **32a** or **32** co-deposited

with cesium (Cs) as the electron transport material (ETM), using the device configuration [ITO/ PEDOT:PSS/  $\alpha$ -NPD/ Alq<sub>3</sub>/ ETM:Cs /Al]. The device with **32b** as the ETM performed the best; with a luminance of 1000 cd m<sup>-2</sup>, driving voltage of 5.0 V, luminance efficiency of 1.8 lm W<sup>-1</sup>, and a current efficiency of 2.8 cd A<sup>-1</sup>. Although more research in this area needs to be accomplished, this shows the potential for using  $\pi$ -conjugated phospholes as electron transporting materials.

### Phosphole based host for OLEDs

The role of a host in phosphorescent OLEDs is to prevent triplet-triplet annihilation in the emissive material. In particular, this matrix needs to have balanced charge transport (to carry both holes and electrons) and a suitable triplet energy level to transfer energy to the triplet emitter. It needs also to possess chemical, thermal and electrochemical stability.

In 2012, Chi/Chou/Chang *et al.* synthesized Osmium (II) metal complexes **33a,b** (Figure 15) that exhibited orange or red phosphorescence with high luminescence quantum yields.<sup>48</sup> In order to explore the full potential of their Os(II) triplet emitters, they decided to develop a specific host material for the fabrication of OLEDs. They synthesized a new bipolar  $\pi$ -conjugated host material that contains a carbazole moiety (electron donor) and a dibenzophosphole oxide moiety (electron acceptor), 5-[4-[(carbazol-9-yl)phenyl]-dibenzophosphole oxide (**34**) (Figure 15).

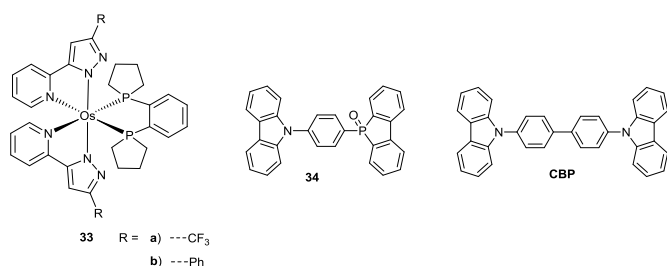


**Figure 15:** Osmium (II) triplet emitters **33** and hosts (**34** and CBP) used in the fabrication of OLEDs.

The bipolar host **34** was synthesized by first generating a dibenzophosphole by a dilithiation of biphenyl, followed by reaction with PhPCl<sub>2</sub> (Figure 16). Then, they cleaved the P-Ph bond with lithium and protonated the phospholide with water and acetic acid. Subsequently the 5*H*-benzo[*b*]phosphindole<sup>49</sup> is coupled to 9-(4-bromophenyl)carbazole with a Cu catalyst, and then oxidized to give **34**.

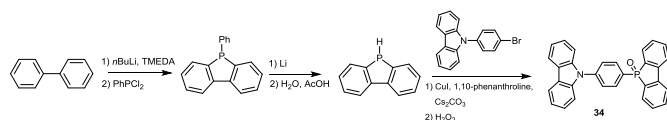


**Figure 16:** Synthesis of compound **34**.

They constructed OLED devices and compared the performances of the OLEDs when they include the Os(II)

complexes in two different hosts: compound **34** and another bipolar host : 4,4'-*N,N'*-dicarbazolebiphenyl (CBP). Using the device configuration [ITO/2,2'-bis(3-(*N,N*-di-*p*-tolylamino)phenyl)-biphenyl (3DTAPBP, hole-transporting layer)/host doped with 4 wt.% of Os complex/3,3'-5,5'-tetra[(*m*-pyridyl)phen-3-yl]biphenyl (BP4mPy, ETL)/LiF/Al], they found that better efficiencies were obtained when the compound **34** was used as the host emitting layer. The device with **33a** in the CBP host had an EL efficiency of 10.9%, current efficiency of 21.7 cd A<sup>-1</sup>, luminance efficiency of 11.9 lm W<sup>-1</sup>, turn-on voltage of 4.3V, and a maximum luminance 19,797 cd m<sup>-2</sup> (21.6 V). But the same compound **33a** in the **34** host had an EL efficiency of 14.3%, current efficiency of 34.8 cd A<sup>-1</sup>, luminance efficiency of 45.2 lm W<sup>-1</sup>, turn-on voltage of 2.5 V, and a maximum luminance 52,624 cd m<sup>-2</sup> (14.2 V). They emphasize that the results of the higher current density and better carrier balance at higher voltages are due to the great carrier transport property of **34**. This example highlights the great potential for utilizing bipolar  $\pi$ -conjugated phosphole oxides as hosts in OLEDs.

### Photovoltaic cells (Organic solar cells (OSCs) and Dye-sensitized Solar Cells (DSSCs))

Fossil fuel alternatives, such as harvesting energy directly from sunlight using photovoltaic technology are one of the way to address growing global energy needs.<sup>50</sup> Since the discovery of silicon solar cell in the 1950's, tremendous advances in solar cell research and development have been made. DSSCs and OSCs devices are promising alternatives for producing clean and renewable energy due to the fact that there is the potential to fabricate them onto large areas of lightweight flexible substrates by solution processing at a low cost.

Generally, *n*-DSSC<sup>51</sup> device consists of four main components: a photoanode of transparent fluorine-doped tin oxide (FTO) glass covered with a wide band gap nanocrystalline *n*-type semiconductor (TiO<sub>2</sub>, ZnO, SnO<sub>2</sub>, Nb<sub>2</sub>O<sub>5</sub>, etc.), a sensitizer (dye molecules, usually a push-pull organic dye or coordination complex) anchored on the surface of the semiconductor, a redox-coupled electrolyte (cobalt complexes, I<sup>-</sup>/I<sub>3</sub><sup>-</sup>...) and a counter electrode of FTO coated with platinum nanoparticles (Figure 17). Under irradiation, the dye molecules chemisorbed on the surface of the semiconductor are excited to create exciton pairs which are rapidly split at the nanocrystalline surface. The electrons are injected into the conduction band of the semiconductor and the holes staying on the dyes are recovered by the redox mediator in the liquid electrolyte. The oxidation state of the redox mediator is further recovered by electrons transferred from the counter electrode. A closed circuit is thereby established to continuously convert the solar light to electricity.

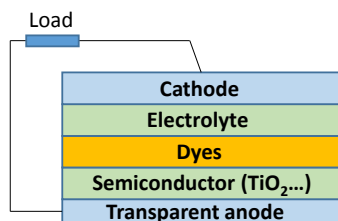


Figure 17: DSSCs structure

If the two semiconductors (n and p-type) are fully organic, the device is referred as OSC. A bulk heterojunction OSC device consists of an active layer composed of a nanoscale blend of donor and acceptor materials sandwiched between two electrodes having different work functions (Figure 18).<sup>8,52</sup> The general working principle first involves the photoexcitation of the donor material by the absorption of light energy to generate excitons. After the exciton dissociation/charge separation process at the donor–acceptor interface, the separated electrons and holes move towards their respective electrodes, driven by either the built-in electric field or the charge carrier concentration gradient, leading to a photocurrent or photovoltage.

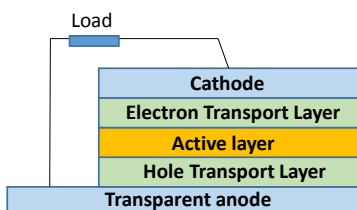


Figure 18: Structure of a bulk heterojunction OPV device.

For an organic material to be suited for SC applications, the material must fulfill certain requirements. He must simultaneously possess strong absorption ability in the visible-near infrared spectral range, suitable HOMO-LUMO energy levels to transfer electrons to n-type semiconductor (or p-type in the case of an acceptor), high hole or electron mobility and good film-forming properties in the case of OSC. Like for the OLEDs, additional charge transport layer (such as ETL or cathode buffer layer) can be inserted in the devices.

### Phosphole based dyes for Dye-sensitized Solar Cells (DSSCs).

The first example of a  $\pi$ -conjugated phosphole for use in a DSSC was described by Matano/Imahori *et al* in 2010.<sup>53</sup> They showed that 1-hydroxy-1-oxodithienophospholes **35a,b** (Figure 19) could serve as a novel anchoring group to the TiO<sub>2</sub> electrode in the DSSC device. It should be mentioned that phosphonates (R-PO<sub>3</sub>H<sub>2</sub>) have already been successfully used as anchoring groups in DSSCs.<sup>54</sup> 1-Hydroxy-1-oxodithienophospholes **35a,b** (Figure 19) were synthesized by first generating the dithienophosphole<sup>55</sup>, which was then treated with NBS to generate the dibromothienophosphole, followed by a Stille coupling to extend the  $\pi$ -conjugation of the system, and finally treated with aqueous HCl to give the corresponding  $\pi$ -conjugated phosphinic acids **35a,b** (Figure 19).

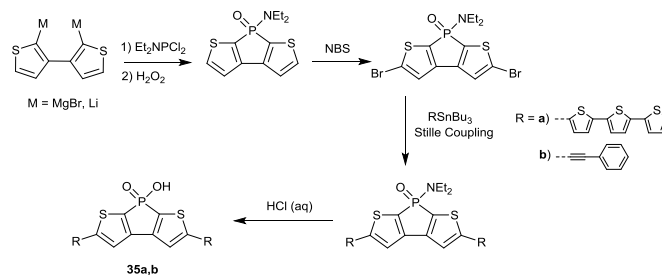
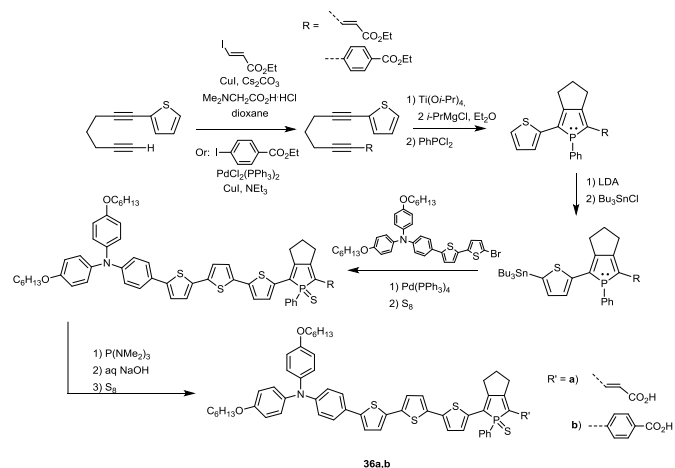


Figure 19: Synthesis of 1-Hydroxy-1-oxodithienophospholes **35a,b**.

DFT calculations showed that the LUMO of **35a,b** are extended to the phosphinic acid group due to an effective  $\sigma^*-\pi^*$  orbital interaction, therefore, they expected a fast electron injection from the dye excited state to the conduction band of the TiO<sub>2</sub> through the anchoring group (POOH). The device configuration consisted of a sandwich cell with the phosphole sensitized on mesoporous P-25 TiO<sub>2</sub> as the working electrode and a platinum conducting glass as the counter electrode. The electrodes were separated by a thin transparent film of Surlyn polymer (Dupont) acting as a spacer for the electrolyte (LiI (0.5M) and I<sub>2</sub> (0.01M) in acetonitrile). The current-voltage characteristics of the devices were evaluated under standard AM 1.5 conditions (100 mW cm<sup>-2</sup>). The device using **35a** as the sensitizer, had a short-circuit current density ( $J_{sc}$ ) of 7.4 mA cm<sup>-2</sup>, an open-circuit voltage ( $V_{oc}$ ) of 0.46V, a fill factor ( $FF$ ) of 0.54, and a power conversion efficiency ( $\eta$ ) of 1.8%. The device using **35b** as the sensitizer, had a  $J_{sc}$  of 2.3mA cm<sup>-2</sup>, an  $V_{oc}$  of 0.44V, a  $FF$  of 0.54, and a  $\eta$  of 0.56%. The TiO<sub>2</sub>/**35a** electrode displayed a maximum incident photon-to-current efficiency (IPCE) of 66% at 400 nm, while the TiO<sub>2</sub>/**35b** had a IPCE of 43% at 400 nm. These results showed two things: i)  $\pi$ -conjugated phosphole phosphinic acids could serve as unique anchoring groups in DSSCs, ii) playing with the  $\pi$ -conjugated substituents attached to the phosphole could enhance the performance of the device.

In 2014, Matano/Imahori *et al.* synthesized new donor- $\pi$ -acceptor organic dyes for DSSCs.<sup>56</sup> The dyes consisted of a triarylamine donor, an oligothiophene  $\pi$  system, a phosphole sulfide as the acceptor unit, and a carboxylic acid anchoring group (Figure 20). The synthesis of these phosphole dyes consists of first synthesizing the disubstituted-bis-alkyne, then using the Sato method<sup>57</sup> for generation of a titanocyclopentadiene which react with PhPCl<sub>2</sub> to form the phosphole (Figure 20). Then, the stannylthiophene is generated and a Stille coupling is performed with a triarylamine-appended 5-bromo-2,2'-bithiophene (Figure 20). In the final step, the carboxylate esters are deprotected into the carboxylic acids **36a,b** (Figure 20).



**Figure 20:** Synthesis of donor- $\pi$ -acceptor phosphole dyes **36a,b** in DSSCs

The fabricated devices have the following structure: [fluorine-doped tin oxide, FTO glass/TiO<sub>2</sub>/ phosphole dye/Surlyn polymer gasket (DuPont)/electrolyte solution/platinum/FTO]. The electrolyte solution used was a mixture of 1,3-dimethylimidazolium iodide (1.0 M), I<sub>2</sub> (0.06 M), LiI (0.05 M), guanidinium thiocyanate (0.1 M), and 4-*tert*-butylpyridine (0.50 M) in acetonitrile. The device incorporating **36a** as a dye, had a  $J_{sc}$  of 9.0 mA cm<sup>-2</sup>, an  $V_{oc}$  of 0.61 V, a FF of 0.68, and a  $\eta$  of 3.7%. The device incorporating **36b** as a dye, had a  $J_{sc}$  of 12.5 mA cm<sup>-2</sup>, an  $V_{oc}$  of 0.63 V, a FF of 0.70, and a  $\eta$  of 5.6%. The TiO<sub>2</sub>/**36a** electrode displayed an IPCE of 52% at 460 nm, while the TiO<sub>2</sub>/**36b** had a IPCE of 79% at 490-500 nm. To date, a power conversion efficiency of 5.6% is the highest  $\eta$  value reported for a phosphole-containing DSSC. These results emphasize the potential utility of  $\pi$ -conjugated phospholes as acceptors in donor- $\pi$ -acceptor sensitizers.

### Phosphole based polymers for organic solar cells (OSC)

In 2014, Matano *et al.* also synthesized copolymers incorporating  $\pi$ -conjugated phospholes to be used in a bulk heterojunction OSC.<sup>58</sup> This work stemmed from Matano's work on 2,5-distannylphospholes for making poly-(phosphole *P*-oxide)<sup>59</sup> and poly(phosphole *P*-imide)s<sup>60</sup>. They first synthesized the 2,5-distannylphosphole, using the Ti-mediated cyclization method (Figure 21),<sup>57</sup> next they oxidized the phosphole with corresponding desired function (either P<sup>V</sup>= NSO<sub>2</sub>C<sub>8</sub>H<sub>17</sub> or P<sup>V</sup>= O). Then, they performed Stille coupling reactions with benzodithiophene derivatives to give the corresponding copolymers **37,38** (Figure 21).

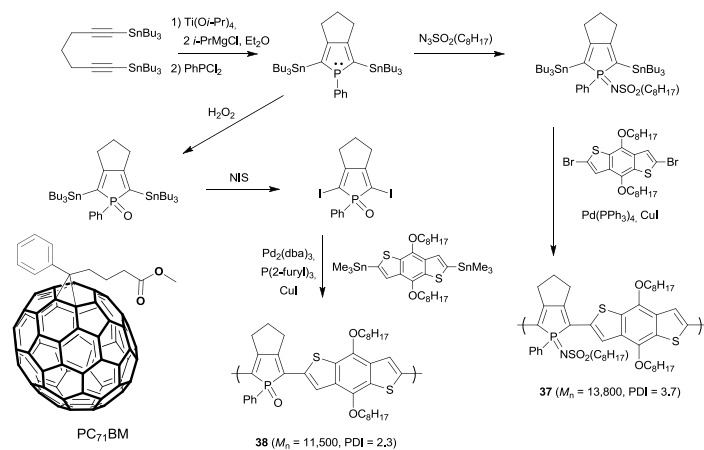


**Figure 21:** Synthesis of phosphole- and benzodithiophene-based copolymers used in OPV devices.

They assembled bulk heterojunction OSC devices having the following configuration [ITO/PEDOT:PSS/polymer:PC<sub>71</sub>BM/Al]. The deposition of the active layer was done by spin-coating a mixture of the polymer (7.2 mg mL<sup>-1</sup>) and PC<sub>71</sub>BM (14.4 mg mL<sup>-1</sup>) over the PEDOT:PSS layer. The device using polymer **37**, had a  $J_{sc}$  of 0.45 mA cm<sup>-2</sup>, an  $V_{oc}$  of 0.45 V, a FF of 0.35, and a  $\eta$  of 0.07%. The device using polymer **38**, had a  $J_{sc}$  of 2.6 mA cm<sup>-2</sup>, an  $V_{oc}$  of 0.63 V, a FF of 0.40, and a  $\eta$  of 0.65%. The difference in the performance of the devices is believed to be that the  $\pi$ -network of polymer **38** device is more densely packed and thus transports the charge carriers more effectively. Although the power conversion efficiencies are not very high, it is indeed interesting to see that changing the substituent of the phosphorus from P<sup>V</sup>= NSO<sub>2</sub>C<sub>8</sub>H<sub>17</sub> to P<sup>V</sup>= O, led to an increase of the  $\eta$  by 9 times. This emphasizes how the substituents on the phosphorus may make a large impact on the charge-generation efficiency and/or charge carrier pathways in the blended films, and thus offers the ability to tune the properties of the system.

In 2015, Park/Kwon/Kim *et al.* demonstrated the great potential of  $\pi$ -conjugated phospholes for use in bulk heterojunction OSC devices, by constructing high-performance solar cells utilizing copolymers based on benzodithiophene and dithienophosphole oxide.<sup>61</sup> They reacted (3,3'-Dibromo-4,4'-didodecyl-[2,2'-bithiophene]-5,5'-diyl)bis(trimethylsilane)<sup>62</sup> with *n*BuLi (Figure 22), followed by the reaction with PhPCl<sub>2</sub>, and subsequent oxidation with hydrogen peroxide to generate the dithienophosphole oxide. Then the reaction with NBS generates terminal bromo groups. Finally, the two novel polymers were generated via Stille coupling polymerization with the corresponding benzodithiophene (Figure 22).

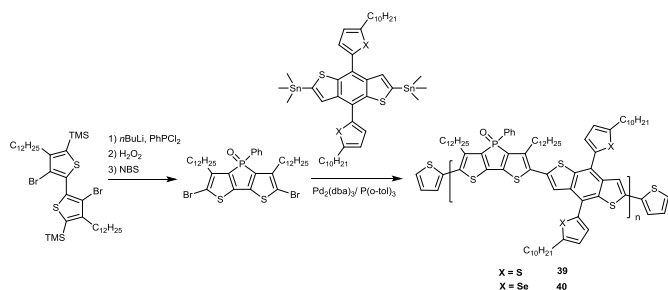


Figure 22: Synthesis of polymers **39** and **40**.

The difference in the two polymers is based on different substituents present on the benzodithiophene unit (i.e. thiophene or selenophene). The ( $M_n$ ) number-average molecular weight of **39** and **40** were 22,000 and 35,000 g mol<sup>-1</sup>, and their PDIs were 1.86 and 1.80, respectively. The authors constructed bulk-heterojunction solar cells with the following structure [ITO/PEDOT:PSS/polymer **39** or **40**:PC<sub>71</sub>BM (1:4, weight ratio)/Ca/Al]. The best performing devices utilized 1,8-octanedithiol (ODT) as a processing additive (0.5% vol). The device utilizing polymer **39** had an  $V_{oc}$  of 0.87V, a  $J_{sc}$  of 13.2 mA cm<sup>-2</sup>, a FF of 53.1%, and a PCE of 6.10%. The device utilizing polymer **40** had an  $V_{oc}$  of 0.85V, a  $J_{sc}$  of 14.8 mA cm<sup>-2</sup>, a FF of 56.3%, and a power conversion efficiency (PCE) of 7.08%. The authors conducted DFT calculations of the dipole moments for both the ground and excited states of the monomers used to build **39** and **40**, and explain that the polarizable dithienophosphole oxide moiety significantly contributes to the very high excited state dipole moment, and leads to efficient charge transfer to the PCBM. The **40** copolymer is currently the best performing dithienophosphole oxide based material for polymer solar cells.

So far, all of the examples of  $\pi$ -conjugated phospholes used in OSC devices that have been described, incorporate the phosphole derivatives as the donor in the device. However, the unique and interesting properties of  $\pi$ -conjugated phospholes could also allow them to be used as acceptors in OSC devices as well.<sup>61,63</sup> We can expect to see future development of  $\pi$ -conjugated phospholes as donors and possibly acceptors in OSCs.

### Phosphole based systems as the cathode buffer layer in OSC

In 2010, Tsuji/Sato/Nakamura *et al.* investigated the use of  $\pi$ -conjugated benzophosphole oxides and sulfides as a cathode buffer layer (ETL) in photovoltaic devices.<sup>64</sup> In the article, they mention that bathocuproine (BCP) is a widely used cathode buffer layer but BCP has a low glass transition temperature ( $T_g = 62^\circ\text{C}$ ) leading to thermal instability of the devices in which it is incorporated into. They investigated the diastereomeric mixtures (two chiral centers on the P atoms) of **32a,b** (Figure 14) and **41a,b** and BCP (Figure 23) as cathode buffer layer in devices incorporating a porphyrin (donor) and a fullerene (acceptor).

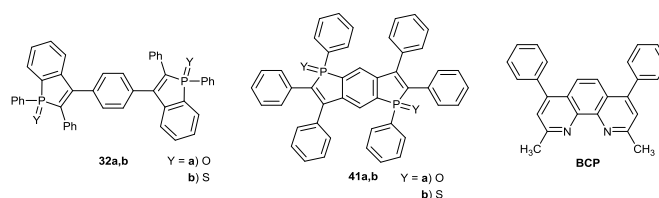


Figure 23: Cathode buffer layers in Tsuji/Sato/Nakamura *et al.* OPV devices.

Phospholes **41a** and **41b** (Figure 24) were synthesized by a previously reported method by Yamaguchi *et al.* which involves an intramolecular *trans*-halophosphanylation of 1,4-dibromo-2,5-bis(phenylethynyl) benzene.<sup>65</sup> Then, a Suzuki coupling with a phenylboronic acid yields phosphole **41a**. Conversion of **41a** to **41b** is possible with the use of Lawesson's reagent (Figure 24).

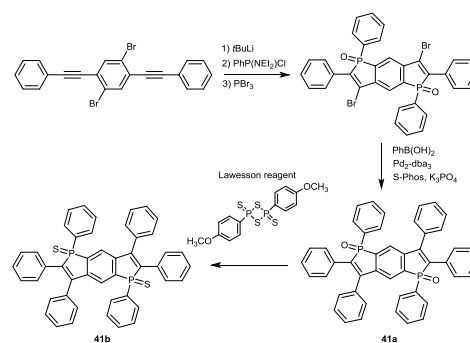
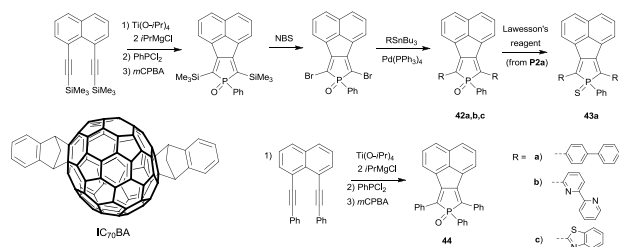


Figure 24: Synthesis of phospholes **41a** and **41b**.

They constructed devices with the following configuration [ITO/PEDOT:PSS/BP/BP:SIMEF/SIMEF/cathode buffer layer/Al]. When they used **32b** as the cathode buffer layer, the device had a PCE of 2.9%, but after annealing (120°C 10 min) the PCE value increased to 4.6%. When they used BCP as the cathode buffer layer they had a PCE of 4.1% but after annealing the PCE dropped dramatically to 0.6%, likely due to the morphological instability of BCP. The performance of the devices using the different phospholes as the cathode buffer layers were similar with the best performances coming from **32b** and **41b**, after annealing. When **41b** was used, the device had an  $V_{oc}$  of 0.72 V, a  $J_{sc}$  of 10.4 mA cm<sup>-2</sup>, a FF of 0.61, and PCE of 4.6%. The phospholes used here as the cathode buffer layer have high morphological stability, represented by their high glass transition temperatures ( $T_g = 148\text{-}159^\circ\text{C}$ ) and their resistance towards crystallization.

In 2012, Matano *et al.* developed a divergent synthesis of  $\alpha,\alpha'$ -diarylacenaphtho[1,2-*c*]phospholes (**42a,b,c**) (Figure 25), which they also incorporated into OSC devices as the cathode buffer layer.<sup>66</sup> This work was an expansion of their previous work on acenaphtho[1,2-*c*]phospholes (e.g. **44**, Figure 25), in 2009.<sup>67</sup> The phospholes were made by reacting 1,8-bis(trimethylsilyl)ethynyl)naphthalene under the Sato method<sup>57</sup> for generation of a titanocyclopentadiene, subsequent metathesis reaction with PPhCl<sub>2</sub>, followed by oxidation to generate the disilylphosphole oxide (Figure 25). Next treatment with NBS cleaves the C-Si bonds and forms C-Br bonds, to yield the dibromophosphole oxide, which then can undergo Stille coupling with stannyl-

derivatives to yield the  $\alpha,\alpha'$ -diarylacenaphtho[1,2-*c*]phospholes (**42a,b,c**). Reaction with Lawesson's reagent converts the phosphole oxide to the phosphole sulphide **43a**.



**Figure 25:** Synthesis of  $\alpha,\alpha'$ -diarylacenaphtho[1,2-*c*]phospholes.

Matano *et al.* found that by modifying the  $\alpha$ -aryl substituents they could tune the degree of  $\pi$ -conjugation, packing motif, electron-accepting ability, and thermal stability of the  $\alpha,\alpha'$ -diarylacenaphtho[1,2-*c*]phospholes. They constructed devices with the following configuration [ITO/PEDOT:PSS/P3HT:IC<sub>70</sub>BA<sup>68</sup> (mixture of regioisomers, 1:0.95; 2.4% weight)/cathode buffer layer/Al] and tested **42a,b,d**, **43a** and BCP as cathode buffer layers, as well as no buffer layer at all. When no buffer layer was used the device had a PCE of 0.9%. When BCP was used as buffer layer the PCE increased to 3.7%. When the phospholes were used the PCE were 2.5% (**43a**), 3.5% (**42b**), 3.7% (**42d**), and 4.2% (**42a**). Thus the best performing device was the one incorporating **42a** as cathode buffer layer ( $V_{OC} = 0.76$  V,  $J_{SC} = 8.8$  mA cm<sup>-2</sup>,  $FF = 0.62$ ). These findings from Tsuji *et al.* and Matano *et al.* highlight the potential of arene-fused phospholes oxides and sulfides as *n*-type semiconductor for organic electronics.

## Other devices

### Electrochromic device

In 2011, Baumgartner/Rodríguez-López *et al.* synthesized and characterized a new class of dendritic structures around a  $\pi$ -conjugated phosphole (Figure 26).<sup>69</sup> These compounds have a rigid  $\pi$ -conjugated phosphole moiety as well as flexible dendritic moieties in order to have supramolecular self-assembling characteristics. These  $\pi$ -conjugated organophosphorus species behaved as organogels and in the absence of solvent as liquid crystals (LC).

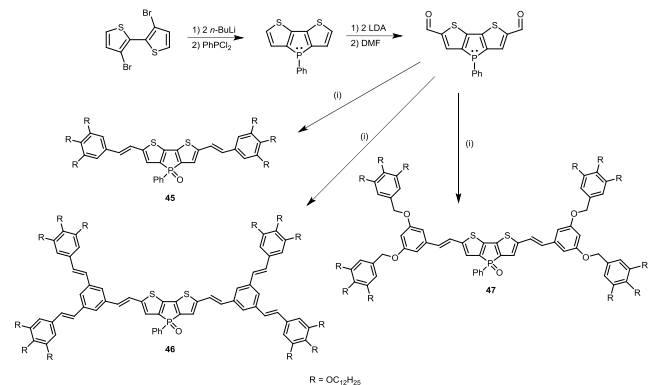


**Figure 26:** Synthesis of dendritic structures around dithieno[3,2-*b*:2',3'-*d*]phospholes. (i) 1. Ar-CH<sub>2</sub>-P(O)(OEt)<sub>2</sub>, *t*BuOK, then H<sub>2</sub>O<sub>2</sub>.

The synthesis (Figure 26) starts from 3,3'-dibromo-2,2'-dithiophene, which is then reacted with 2 equiv. of *n*BuLi to perform a lithium-halogen exchange. Then PPhCl<sub>2</sub> is added to reaction mixture for generating the phosphole ring.<sup>41a</sup> The dithieno[3,2-*b*:2',3'-*d*]phosphole is then reacted with LDA followed by the reaction with DMF to form the diformyl-dithieno[3,2-*b*:2',3'-*d*]phosphole.<sup>70</sup> From there the desired dendrimers are attached *via* Wittig-Horner coupling reactions between aldehydes and phosphonates. These organophosphorus dendritic structures **45-47** were emissive in solution (photoluminescence, quantum yields = 22-24%), but also show strong photoluminescence in the solid state with emission maxima in the orange-red region (585-599 nm). These compounds also exhibited solvato(fluoro)chromism. Thermal studies of compounds **45-47** found that they could self-assemble into supramolecular entities that generate LC columnar arrangements. Based on the color tenability, the solid state photoluminescence and the adequate redox potentials of these compounds, the authors decided to look at the electrochromic properties of phosphole **46**. Electrochromism is the phenomenon displayed by some materials that involves the change of optical properties of the material once a potential is applied. The authors constructed a device having the following configuration [ITO/ compound **46**/electrolyte (Bu<sub>4</sub>NClO<sub>4</sub>/THF 0.1M)/ITO]. Upon applying a potential greater than 1.6 V, the photoluminescence of the thin film under a UV-light changed from an orange emission to a light-green one. This was the first time that electrochromic characteristics were studied with a phosphorus heterocycle. This work shows the potential application of these multifunctional  $\pi$ -conjugated phosphole materials, which can be new candidates for devices such as optical switches.

In 2015, Baumgartner *et al.* published two articles in which they synthesized phosphaviologens and incorporated them into multicolored electrochromic devices.<sup>71</sup> Viologens are bipyridinium derivatives of 4,4'-bipyridyl, which are known for undergoing reversible redox chemistry at low potential in which three differently colored oxidation states exist (e.g. colorless, purple, and orange/red).<sup>72</sup> The synthesis of these phosphaviologens first begins with the synthesis of 2,7-diazadibenzophosphole oxide, **48**, which was reported by Baumgartner in 2011.<sup>73</sup>

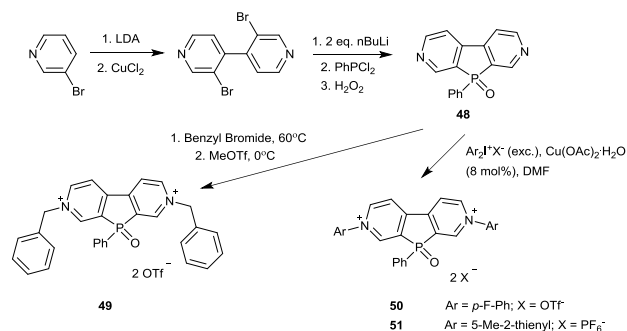


**Figure 27:** Synthesis of phosphaviologens.

Starting from 3-bromopyridine, an Ullmann<sup>74</sup> coupling is performed with LDA and CuCl<sub>2</sub> to give the 3,3'-dibromo-4,4'-bipyridine (Figure 27). Next the 3,3'-dibromo-4,4'-bipyridine is reacted with nBuLi and PPhCl<sub>2</sub>, followed by oxidation of the phosphorus with hydrogen peroxide to give the 2,7-diazadibenzophosphole oxide. Finally the phosphaviologens could be produced upon diquaternization of the two nitrogen centers with the corresponding reagents to give the *N*-benzylated<sup>71a</sup> or *N*-arylated<sup>71b</sup> phosphaviologens.

The authors constructed a proof-of-concept device with their *N*-benzylated<sup>71a</sup> phosphaviologens (**49**, Figure 27) consisting of two fluorine-doped tin oxide (FTO)-coated glass electrodes, then sealed together with a UV-cured gasket using a hardware gel, containing a solution of the phosphaviologen. Applying 0.1V potential to the device resulted in the conversion of the colorless (dication) to the blue/violet (radical cation). The process could be reversed over time by the diffusion of air into the cell. This first device was not very reversible due to the build up of the strongly colored radical on the opposite electrode. A modified device where the FTO was partially removed from each side of the glass before sealing, could prevent the build up of the strongly colored radical on the opposite electrode. Then, alternating between positive and negative potentials their device displayed electrochromism reversibility, alternating between colorless (dication) and blue/violet (radical cation). It should be mentioned that they never observed complete discoloration, this was due to the cell thickness, and that the colored radical species would diffuse through the solution at a rate faster than the potential switching.

The authors also constructed a similar device with their *N*-arylated<sup>71b</sup> phosphaviologens. It consisted of two FTO-coated glass plates sandwiching an acetonitrile solution of the respective compound (**50** and **51**). When a potential difference of 0.1V was applied to the glass electrodes, a complete color change occurred corresponding to the radical cation of each. Applying a higher voltage (0.4V) the color changed again as the neutral species is formed. The process is reversed over time by the diffusion of air into the cell. The redox states could also be achieved chemically for comparison. In the case of the thienyl substituted phosphaviologen (**51**), because of the diminished energy gap and absorption in the visible range of the dication form, efficient switching between yellow and purple colors was possible, which had not been achieved for viologens yet. This is the first example of a phosphaviologen that can switch between colors for all three states. It should be mentioned that the presence of the central five-membered phosphole oxide ring doesn't significantly alter the redox behavior and electrochromic properties of the phosphaviologens compared to methyl viologen, yet significantly lowers the reduction threshold for both redox steps, and allows for tuning of the LUMO levels of these compounds. These examples highlight the potential of these  $\pi$ -conjugated phosphorus species for applications such as dimming devices and multicolored displays.

## Conclusions

$\pi$ -Conjugated phospholes have many unique favorable properties that have applications in organic electronic materials. These include: (i) their weak aromaticity, (ii) substitution about the phosphole can influence their aromaticity, (iii) have an efficient overlap between the  $\sigma$  orbitals of the exocyclic P-R bond and the  $\pi$ -orbitals from the endocyclic dienic system offering an original mode of conjugation, (iv) a versatile synthesis allowing tuning the  $\pi$ -systems, the aliphatic chains and the grafting unit; (v) have a reactive phosphorus lone pair, which can be used to tune the physicochemical properties of the  $\pi$ -conjugated system using simple chemical modification (oxidation, alkylation, or coordination), (vi) a pyramidal P-atom that prevent aggregation in the solid state and promote solid-state fluorescence.

While this review focuses on  $\pi$ -conjugated phospholes incorporated into devices, there are still many other interesting and exciting  $\pi$ -conjugated phosphole materials<sup>17,22</sup> that have yet to be incorporated into devices. Furthermore, most of the compounds presented in this review are prepared through Sato/Fagan-Nugent heterole synthesis of corresponding alkyne or via lithiation of dihaloaromatic precursors. However, the fast development of transition metal-catalyzed phosphole synthesis might lead to the preparation of unprecedented  $\pi$ -conjugated systems.<sup>75</sup> Although there is still more work to be done, this review serves as a stepping stone to reiterate what devices have been done and to envision where to go from here. Keep in mind; several of the devices described here are still not fully optimized. There is little doubt that in the next few years, more and more phosphole containing materials will be incorporated into devices like organic light emitting diodes (OLED), organic field effect transistors (OFET), organic photovoltaic cells (OPV), and other devices as well.

## Acknowledgements

This work is supported by the Ministère de la Recherche et de l'Enseignement Supérieur, the CNRS, the Région Bretagne, China-French associated international laboratory in "Functional Organophosphorus Materials", the French National Research Agency (ANR)/Research Grants Council (RGC) Joint Research Scheme (ANR MOLMAT) and COST CM10302 (SIPS).

## Notes and References

‡ Footnotes relating to the main text should appear here. These might include comments relevant to but not central to the matter under discussion, limited experimental and spectral data, and crystallographic data.

- 1 F. Wudl, D. Wobschall and E. J. Hufnagel, *J. Am. Chem. Soc.*, 1972, **94**, 670.
- 2 (a) H. Shirakawa, E. J. Louis, A. G. Macdiarmid, C. K. Chiang and A. J. Heeger, *J. Chem. Soc., Chem. Commun.*, 1977, 578; (b) C. K.

- Chiang, C. R. Fincher, Y. W. Park, A. J. Heeger, H. Shirakawa, E. J. Louis, S. C. Gau and A. G. Macdiarmid, *Physical Review Letters*, 1977, **39**, 1098.
- 3 A. Kraft, A. C. Grimsdale and A. B. Holmes, *Angew. Chem. Int. Ed.*, 1998, **37**, 402.
  - 4 (a) A. F. Diaz, K. K. Kanazawa and G. P. Gardini, *J. Chem. Soc., Chem. Commun.*, 1979, 635; (b) M. Sun, L. Wang and W. Yang, *Journal of Applied Polymer Science*, 2010, **118**, 1462.
  - 5 O. Gidron and M. Bendikov, *Angew. Chem. Int. Ed.*, 2014, **53**, 2546.
  - 6 (a) J. Roncali, *Chem. Rev.*, 1997, **97**, 173; (b) A. Mishra, C.-Q. Ma and P. Bäuerle, *Chem. Rev.* 2009, **109**, 1141
  - 7 (a) S. Yamaguchi and K. Tamao, *J. Chem. Soc. Dalton Trans.*, 1998, 3693; (b) M. Hissler, P. W. Dyer and R. Réau, *Coord. Chem. Rev.*, 2003, **244**, 1; (c) X. Zhan, S. Barlow and S. R. Marder, *Chem. Commun.*, 2009, 1948.
  - 8 (a) K. Müllen and G. Wegner, *Electronic Materials : The Oligomer Approach*, Wiley-VCH, Weinheim, 1998; (b) T. A. Skotheim and J. R. Reynolds, *Handbook of conducting polymers*, CRC, Boca Raton, Fla., 2007; (c) B. C. Thompson and J.M.J. Fréchet, *Angew. Chem. Int. Ed.* 2008, **47**, 58. (d) J. L. Delgado, P.-A. Bouit, S. Fillipone, M.A. Herranz and N. Martín, *Chem. Commun.* 2010, **46**, 4853.
  - 9 (a) G. Li, V. Shrotriya, J. S. Huang, Y. Yao, T. Moriarty, K. Emery and Y. Yang, *Nature Mater.*, 2005, **4**, 864; (b) B. L. Groenendaal, F. Jonas, D. Freitag, H. Pielartzik and J. R. Reynolds, *Adv. Mater.*, 2000, **12**, 481.
  - 10 (a) H. Sirringhaus, N. Tessler and R. H. Friend, *Science*, 1998, **280**, 1741; (b) J. F. Chang, B. Q. Sun, D. W. Breiby, M. M. Nielsen, T. I. Solling, M. Giles, I. McCulloch and H. Sirringhaus, *Chem. Mat.*, 2004, **16**, 4772; (c) H. Sirringhaus, T. Kawase, R. H. Friend, T. Shimoda, M. Inbasekaran, W. Wu and E. P. Woo, *Science*, 2000, **290**, 2123.
  - 11 (a) P. A. Levermore, L. C. Chen, X. H. Wang, R. Das and D. D. C. Bradley, *Adv. Mater.*, 2007, **19**, 2379; (b) M. Heo, J. Kim, J. Y. Kim and C. Yang, *Macromol. Rapid Commun.*, 2010, **31**, 2047.
  - 12 (a) E. H. Braye and W. Hübel, *Chem. Ind. (London)*, 1959, 1250; (b) E. H. Braye, I. Caplier and W. Hübel, *J. Am. Chem. Soc.*, 1961, **83**, 4406; (c) F. C. Leavitt, T. A. Manuel and F. Johnson, *J. Am. Chem. Soc.*, 1959, **81**, 3163.
  - 13 (a) F. Mathey, *Chem. Rev.*, 1988, **88**, 429; (b) M. O. Bevierre, F. Mercier, L. Ricard and F. Mathey, *Angew. Chem. Int. Ed.*, 1990, **29**, 655; (c) E. Deschamps, L. Ricard and F. Mathey, *Heteroatom Chemistry*, 1991, **2**, 377.
  - 14 W. Schäfer, A. Schweig and F. Mathey, *J. Am. Chem. Soc.*, 1976, **98**, 407.
  - 15 R. Szúcs, P.-A. Bouit, M. Hissler and L. Nyulaszi, *Struct. Chem.*, 2015, **26**, 1351.
  - 16 C. Charrier, H. Bonnard, G. Delauzon and F. Mathey, *J. Am. Chem. Soc.*, 1983, **105**, 6871.
  - 17 R. Réau and T. Baumgartner, *Chem. Rev.*, 2006, **106**, 4691.
  - 18 (a) P. v. R. Schleyer, P. K. Freeman, H. J. Jiao and B. Goldfuss, *Angew. Chem. Int. Ed.*, 1995, **34**, 337; (b) L. D. Quin, in *Comprehensive Heterocyclic Chemistry II*, eds. A. R. Katritzky, C. W. Rees and E. F. V. Scriven, Elsevier, Oxford, 1996, pp. 757-856; (c) P. V. Schleyer, C. Maerker, A. Dransfeld, H. J. Jiao and N. Hommes, *J. Am. Chem. Soc.*, 1996, **118**, 6317; (d) D. Delaere, A. Dransfeld, M. T. Nguyen and L. G. Vanquickenborne, *J. Org. Chem.*, 2000, **65**, 2631; (e) L. Nyulaszi, *Chem. Rev.*, 2001, **101**, 1229; (f) E. Mattmann, F. Mathey, A. Sevin and G. Frison, *J. Org. Chem.*, 2002, **67**, 1208; (g) M. K. Cyranski, T. M. Krygowski, A. R. Katritzky and P. V. Schleyer, *J. Org. Chem.*, 2002, **67**, 1333.
  - 19 L. Nyulaszi, O. Holloczki, C. Lescop, M. Hissler and R. Réau, *Org. Biomol. Chem.*, 2006, **4**, 996.
  - 20 (a) D. Delaere, M. T. Nguyen and L. G. Vanquickenborne, *J. Phys. Chem. A*, 2003, **107**, 838; (b) E. Mattmann, D. Simonutti, L. Ricard, F. Mercier and F. Mathey, *J. Org. Chem.*, 2001, **66**, 755. (c) S. A. Katsyuba, T. I. Burganov, E. E. Zvereva, A. A. Zagidullin, V. A. Miluykov, P. Lonneck, E. Hey-Hawkins and O. G. Sinyashin, *J. Phys. Chem. A*, 2014, **118**, 12168
  - 21 (a) L. D. Quin, G. Keglevich, A. S. Ionkin, R. Kalgutkar and G. Szalontai, *J. Org. Chem.*, 1996, **61**, 7801; (b) L. Nyulaszi, G. Keglevich and L. D. Quin, *J. Org. Chem.*, 1996, **61**, 7808; (c) G. Keglevich, Z. Bocskei, G. M. Keseru, K. Ujszaszy and L. D. Quin, *J. Am. Chem. Soc.*, 1997, **119**, 5095.
  - 22 (a) L. D. Quin, in *Phosphorus-Carbon Heterocyclic Chemistry*, ed. F. Mathey, Elsevier Science Ltd, Oxford, 2001, pp. 219-305; (b) L. D. Quin and G. S. Quin, in *Phosphorus-Carbon Heterocyclic Chemistry*, ed. F. Mathey, Elsevier Science Ltd, Oxford, 2001, pp. 307-362; (c) Y. Matano and H. Imahoria, *Org. Biomol. Chem.*, 2009, **7**, 1258; (d) A. A. Zagidullin, I. A. Bezkishko, V. A. Miluykov and O. G. Sinyashin, *Mendeleev Commun.*, 2013, **23**, 117.
  - 23 J. Crassous and R. Réau, *Dalton Trans.*, 2008, 6865.
  - 24 C. Hay, C. Fischmeister, M. Hissler, L. Toupet and R. Réau, *Angew. Chem. Int. Ed. Engl.*, 2000, **39**, 1812. C. Hay, M. Hissler, C. Fischmeister, J. Rault-Berthelot, L. Toupet, L. Nyulaszi and R. Réau, *Chem.-Eur. J.*, 2001, **7**, 4222.
  - 25 P.-A. Bouit, A. Escande, R. Szucs, D. Szieberth, C. Lescop, L. Nyulaszi, M. Hissler and R. Réau, *J. Am. Chem. Soc.*, 2012, **134**, 6524.
  - 26 (a) S. O. Jeon and J. Y. Lee, *J. Mater. Chem.* 2012, **22**, 4233; (b) D. Joly, P.-A. Bouit and M. Hissler, *J. Mater. Chem. C* 2016, **4**, 3686.
  - 27 (a) K. Müllen, U. Scherf, (Eds), *Organic Light Emitting Devices: Synthesis Properties and Applications*, Wiley-VCH, Weinheim, Germany 2006; (b) S. Scholz, D. Kondakov, B. Lüssem, K. Leo, *Chem. Rev.* 2015, **115**, 8449; (c) G. M. Farinola, R. Ragni, *Chem. Soc. Rev.*, 2011, **10**, 3467; (d) A. C. Grimsdale, K. L. Chan, R. E. Martin, P. G. Jokisz and A. B. Holmes, *Chem. Rev.*, 2009, **109**, 897.
  - 28 Some additionnal layers (hole blocking layer, electron blocking layers) can also be inserted to increase the performances
  - 29 C. Fave, T. Y. Cho, M. Hissler, C. W. Chen, T. Y. Luh, C. C. Wu and R. Réau, *J. Am. Chem. Soc.*, 2003, **125**, 9254.
  - 30 K. Sonogashira, Y. Tohda and N. Hagihara, *Tetrahedron Letters*, 1975, 4467.
  - 31 (a) P. J. Fagan and W. A. Nugent, *J. Am. Chem. Soc.*, 1988, **110**, 2310; (b) P. J. Fagan, W. A. Nugent and J. C. Calabrese, *J. Am. Chem. Soc.*, 1994, **116**, 1880.
  - 32 H. C. Su, O. Fadhel, C. J. Yang, T. Y. Cho, C. Fave, M. Hissler, C. C. Wu and R. Réau, *J. Am. Chem. Soc.*, 2006, **128**, 983.
  - 33 D. Joly, D. Tondelier, V. Deborde, B. Geffroy, M. Hissler and R. Réau, *New J. Chem.*, 2010, **34**, 1603
  - 34 O. Fadhel, M. Gras, N. Lemaitre, V. Deborde, M. Hissler, B. Geffroy and R. Réau, *Adv. Mater.*, 2009, **21**, 1261.
  - 35 D. Joly, D. Tondelier, V. Deborde, W. Delaunay, A. Thomas, K. Bhanuprakash, B. Geffroy, M. Hissler and R. Réau, *Adv. Funct. Mater.*, 2012, **22**, 567.

- 36 M. P. Duffy, P.-A. Bouit, B. Geffroy, D. Tondelier and M. Hissler, *Phosphorus, Sulfur, and Silicon and the Related Elements*, 2014, **190**, 845.
- 37 H. Chen, W. Delaunay, L. Yu, D. Joly, Z. Wang, J. Li, Z. Wang, C. Lescop, D. Tondelier, B. Geffroy, Z. Duan, M. Hissler, F. Mathey and R. Réau, *Angew. Chem. Int. Ed.*, 2012, **51**, 214.
- 38 (a) M.-O. Bevierre, F. Mercier, L. Ricard and F. Mathey, *Angewandte Chemie*, 1990, **102**, 672; (b) F. Laporte, F. Mercier, L. Ricard and F. Mathey, *J. Am. Chem. Soc.*, 1994, **116**, 3306.
- 39 (a) M. Gouygou, O. Tissot, J.-C. Daran and G. G. A. Balavoine, *Organometallics*, 1997, **16**, 1008; (b) E. Robé, C. Ortega, M. Mikina, M. Mikolajczyk, J.-C. Daran and M. Gouygou, *Organometallics*, 2005, **24**, 5549.
- 40 R. Kondo, T. Yasuda, Y. S. Yang, J. Y. Kim and C. Adachi, *J. Mater. Chem.*, 2012, **22**, 16810.
- 41 (a) T. Baumgartner, T. Neumann and B. Wirges, *Angew. Chem. Int. Ed.*, 2004, **43**, 6197; (b) T. Baumgartner, W. Bergmans, T. Karpati, T. Neumann, M. Nieger and L. Nyulaszi, *Chem.-Eur. J.*, 2005, **11**, 4687; (c) Y. Dienes, S. Durben, T. Karpati, T. Neumann, U. Englert, L. Nyulaszi and T. Baumgartner, *Chem.-Eur. J.*, 2007, **13**, 7487.
- 42 H. Chen, W. Delaunay, J. Li, Z. Y. Wang, P. A. Bouit, D. Tondelier, B. Geffroy, F. Mathey, Z. Duan, R. Réau and M. Hissler, *Org. Lett.*, 2013, **15**, 330.
- 43 P. Gong, K. Ye, J. Sun, P. Chen, P. Xue, H. Yang and R. Lu, *RSC Adv.*, 2015, **5**, 94990.
- 44 F. Riobé, R. Szucs, P. A. Bouit, D. Tondelier, B. Geffroy, F. Aparicio, J. Buendia, L. Sanchez, R. Réau, L. Nyulaszi and M. Hissler, *Chem. Eur. J.*, 2015, **21**, 6547.
- 45 R. F. Chen, R. Zhu, Q. L. Fan and W. Huang, *Org. Lett.*, 2008, **10**, 2913.
- 46 H. Tsuji, K. Sato, Y. Sato and E. Nakamura, *J. Mater. Chem.*, 2009, **19**, 3364.
- 47 H. Tsuji, K. Sato, L. Ilies, Y. Itoh, Y. Sato and E. Nakamura, *Org. Lett.*, 2008, **10**, 2263.
- 48 C. H. Lin, C. W. Hsu, J. L. Liao, Y. M. Cheng, Y. Chi, T. Y. Lin, M. W. Chung, P. T. Chou, G. H. Lee, C. H. Chang, C. Y. Shih and C. L. Ho, *J. Mater. Chem.*, 2012, **22**, 10684.
- 49 (a) W. Neugebauer, A. J. Kos and P. V. Schleyer, *J. Organometallic Chem.*, 1982, **228**, 107; (b) E. H. Braye, I. Caplier and R. Saussez, *Tetrahedron*, 1971, **27**, 5523; (c) E. Duran, D. Velasco and F. Lopez-Calahorra, *Heterocycles*, 2002, **57**, 825.
- 50 (a) C. J. Brabec, N. S. Sariciftci and J. C. Hummelen, *Adv. Funct. Mater.* 2001, **11**, 15; (b) S. Günes, H. Neugebauer and N. S. Sariciftci, *Chem. Rev.* 2007, **107**, 1324; (c) W. Cao and J. Xue, *Energy Environ. Sci.*, 2014, **7**, 2123; (d) H.-Y. Chen, D.-B. Kuang and C.-Y. Su, *J. Mater. Chem.*, 2012, **22**, 15472.
- 51 (a) M. Grätzel, *Inorg. Chem* 2005, **44**, 6841.; (b) A. Hagfeldt, G. Boschloo, L. Sun, L. Kloo and H. Pettersson, *Chem. Rev.* 2010, **110**, 6595.
- 52 Y.-Y. Cheng, S.-H. Yang, C. S. Hsu, *Chem Rev* 2009, **109**, 5968.
- 53 A. Kira, Y. Shibano, S. Kang, H. Hayashi, T. Umeyama, Y. Matano and H. Imahori, *Chem. Lett.*, 2010, **39**, 448.
- 54 (a) F. Odobel, E. Blart, M. Lagrée, M. Villieras, H. Boujtita, N. El Murr, S. Caramori and C. Alberto Bignozzi, *J. Mater. Chem.*, 2003, **13**, 502; (b) M. K. Nazeeruddin, R. Humphry-Baker, D. L. Officer, W. M. Campbell, A. K. Burrell and M. Grätzel, *Langmuir*, 2004, **20**, 6514.
- 55 V. Vicente, A. Fruchier, M. Taillefer, C. Combes-Chamalet, I. J. Scowen, F. Plenat and H. J. Cristau, *New J. Chem.*, 2004, **28**, 418.
- 56 Y. Matano, Y. Hayashi, H. Nakano and H. Imahori, *Heteroatom Chemistry*, 2014, **25**, 533.
- 57 (a) H. Urabe, K. Suzuki and F. Sato, *J. Am. Chem. Soc.*, 1997, **119**, 10014; (b) H. Urabe, T. Takeda, D. Hideura and F. Sato, *J. Am. Chem. Soc.*, 1997, **119**, 11295.
- 58 Y. Matano, H. Ohkubo, T. Miyata, Y. Watanabe, Y. Hayashi, T. Umeyama and H. Imahori, *Eur. J. Inorg. Chem.*, 2014, **2014**, 1620.
- 59 A. Saito, Y. Matano and H. Imahori, *Org. Lett.*, 2010, **12**, 2675.
- 60 Y. Matano, H. Ohkubo, Y. Honsho, A. Saito, S. Seki and H. Imahori, *Org. Lett.*, 2013, **15**, 932.
- 61 K. H. Park, Y. J. Kim, G. B. Lee, T. K. An, C. E. Park, S.-K. Kwon and Y.-H. Kim, *Adv. Funct. Mater.*, 2015, **25**, 3991
- 62 Z. Fei, Y. Kim, J. Smith, E. B. Domingo, N. Stingelin, M. A. McLachlan, K. Song, T. D. Anthopoulos and M. Heeney, *Macromolecules*, 2012, **45**, 735.
- 63 J. E. Anthony, *Chem. Mater.*, 2011, **23**, 583.
- 64 H. Tsuji, K. Sato, Y. Sato and E. Nakamura, *Chem. Asian J.*, 2010, **5**, 1294.
- 65 A. Fukazawa, Y. Ichihashi, Y. Kosaka and S. Yamaguchi, *Chem. Asian J.*, 2009, **4**, 1729.
- 66 Y. Matano, A. Saito, Y. Suzuki, T. Miyajima, S. Akiyama, S. Otsubo, E. Nakamoto, S. Aramaki and H. Imahori, *Chem. Asian J.* 2012, **7**, 2305.
- 67 A. Saito, T. Miyajima, M. Nakashima, T. Fukushima, H. Kaji, Y. Matano and H. Imahori, *Chem.-Eur. J.*, 2009, **15**, 10000.
- 68 (a) Y. He, G. Zhao, B. Peng and Y. Li, *Adv. Funct. Mater.*, 2010, **20**, 3383; (b) X. Fan, C. Cui, G. Fang, J. Wang, S. Li, F. Cheng, H. Long and Y. Li, *Adv. Funct. Mater.*, 2012, **22**, 585.
- 69 C. Romero-Nieto, M. Marcos, S. Merino, J. Barbera, T. Baumgartner and J. Rodriguez-Lopez, *Adv. Funct. Mater.*, 2011, **21**, 4088.
- 70 C. Romero-Nieto, S. Merino, J. Rodriguez-Lopez and T. Baumgartner, *Chem.-Eur. J.*, 2009, **15**, 4135.
- 71 (a) M. Stolar, J. Borau-Garcia, M. Toonen and T. Baumgartner, *J. Am. Chem. Soc.*, 2015, **137**, 3366; (b) C. Reus, M. Stolar, J. Vanderkley, J. Nebauer and T. Baumgartner, *J. Am. Chem. Soc.*, 2015, **137**, 11710.
- 72 (a) R. J. Mortimer, *Electrochim. Acta*, 1999, **44**, 2971; (b) M. Li, Y. Wei, J. Zheng, D. Zhu and C. Xu, *Org. Electron.*, 2014, **15**, 428.
- 73 S. Durben and T. Baumgartner, *Angew Chem Int Ed Engl*, 2011, **50**, 7948.
- 74 J. Hassan, M. Sévignon, C. Gozzi, E. Schulz and M. Lemaire, *Chem. Rev.*, 2002, **102**, 1359.
- 75 (a) K. Yavari, S. Moussa, B. Ben Hassine, P. Retailleau, A. Voituriez and A. Marinetti, *Angew. Chem. Int. Ed.*, 2012, **51**, 6748 (b) Y. Kuninobu, T. Yoshida and K. Takai, *J. Org. Chem.*, 2011, **76**, 7370; (c) K. Baba, M. Tobisu and N. Chatani, *Angew. Chem.*, 2013, **125**, 12108; (d) Y.-R. Chen and W.-L. Duan, *J. Am. Chem. Soc.*, 2013, **135**, 16754; (e) Y. Unoh, K. Hirano, T. Satoh and M. Miura, *Angew. Chem. Int. Ed.*, 2013, **52**, 12975; (f) Y. Unoh, T. Satoh, K. Hirano and M. Miura, *ACS Catalysis*, 2015, **5**, 6634.